Alma Mater Studiorum – Università di Bologna

DOTTORATO DI RICERCA IN

Meccanica e Scienze Avanzate dell'Ingegneria
Progetto n. 3 – Meccanica Applicata

Ciclo XXIII

Settore/i scientifico-disciplinare/i di afferenza: ING-IND/13

THE POTENTIAL OF THE 3-UPU TRANSLATIONAL PARALLEL MANIPULATOR AND A PROCEDURE TO SELECT THE BEST ARCHITECTURE

Presentata da: **Ing. Ahmed Hachem CHEBBI**

Coordinatore Dottorato

Chiar.mo Prof.
Vincenzo PARENTI CASTELLI

Relatore

Chiar.mo Prof.
Vincenzo PARENTI CASTELLI

Esame finale anno 2011

Dedication

This dissertation is dedicated to my parents for giving me all their love and support throughout graduate school

Keywords:

- *Parallel manipulator*
- *Architecture*
- *Singularity*
- *Clearance*
- *Stiffness*

Abstract

The 3-UPU three degrees of freedom fully parallel manipulator, where U and P are for universal and prismatic pair respectively, is a very well known manipulator that can provide the platform with three degrees of freedom of pure translation, pure rotation or mixed translation and rotation with respect to the base, according to the relative directions of the revolute pair axes.

In particular, pure translational parallel 3-UPU manipulators (3-UPU TPMs) received great attention. Many studies have been reported in the literature on singularities, workspace, and joint clearance influence on the platform accuracy of this manipulator. However, much work has still to be done to reveal all the features this topology can offer to the designer when different architecture, i.e. different geometry are considered.

Therefore, this dissertation will focus on this type of the 3-UPU manipulators. The first part of the dissertation presents new architectures of the 3-UPU TPMs which offer interesting features to the designer. In the second part, a procedure is presented which is based on proposed indexes, in order to allow the designer to select the best architecture of the 3-UPU TPMs for a given task. Some indexes are proposed related to stiffness, clearance, singularity and size of the manipulator in order to apply the procedure.

Contents

List of Figures

List of Tables

Introduction

Parallel manipulators (PMs) have focused a great attention in the last decades for their complementary characteristics with respect to the serial manipulators. Indeed, just to cite a few issues, they exhibit high rigidity, high payload to the manipulator weight ratio, high dynamic performance whilst limited workspace and a low dexterous manipulability. Six degrees of freedom (DOF) PMs have been widely studied. Recently, parallel manipulators (PMs) with less than three degrees of freedom (DOF) have attracted the attention since many tasks do not require 6-DOF and consequently less complex and cheaper machines are worth to be studied.

In particular 3-DOF PMs have been studied in the last two decades mainly after the Delta robot was proposed in 1988 [1]. Many different topologies have been presented since then with various complexities. Three-DOF PMs of pure translation, rotation and a mixed of rotation and translation of the end effector (platform) with respect to the base have been deeply studied and almost all possible topologies have been presented [2-19]. The influence of the topology on the performances of the manipulator has also been investigated. However, much is still to be said, still keeping the same topology, on the influence of the manipulator geometry, i.e. of its architecture, which can change significantly the behaviour of the manipulator.

An interesting 3-DOF PM is the 3-UPU one, presented by Tsai in [4]. Here U and P are for universal and prismatic kinematic pairs respectively. Normally the prismatic pairs are actuated while the remaining ones are passive. This topology that features three serial chains (legs) of type UPU connecting the base with the platform, under certain geometric conditions provides the movable platform with 3 DOF of pure translation with respect to the base. This paper will focus on this family of 3-UPU translational parallel manipulators, hereafter called 3-UPU TPMs.

Since its appearance in [4], the influence of geometry on the 3-UPU TPM performances has been investigated [6,9,12,14,20,21,22], many different architectures presented, and their performances discussed. Moreover, the 3-UPU TPM represented a kind of benchmark mechanism for the study of different type of singularities [8,9,12,14,17,20,21] in parallel manipulators. Nevertheless, further architectures still deserve attention. Indeed, in a recent paper [23], the influence of the location of the legs has been investigated leading to new 3-UPU TPM architectures with interesting features.

The aim of this dissertation is to present new architectures of the 3-UPU TPM in order to show the potential of the 3-UPU topology on one hand, and to propose a procedure that allows the designer to select the best architecture of the 3-UPU TPMs for a given task on the other hand. In particular, the influence of the orientation of the revolute joint axes on the base and on the platform respectively (each universal joint comprises two revolute pairs with intersecting and perpendicular axes), is investigated with special attention to its influence on the singularity loci, and consequently on the manipulator workspace free from singularity. Six new 3-UPU TPM architectures, which can be classified as planar and skew architectures (Planar architectures have the three revolute joint axes connecting the base/platform with the leg coplanar while the skew architectures have these three axes skewed), are presented. These architectures exhibit attractive kinematic and static performances. In addition, two performance indexes are proposed as main tools of the procedure to select the best architecture, also exploiting the size of the manipulator and the definition of singularity can give useful information for the selection. The first proposed index corresponds to the stiffness of the manipulator. The stiffness index is based on the computation of the stiffness matrix that provides a relation between the external wrench applied on the platform and the displacement of the platform itself; the Denavit Hartenberg parameters together with an equivalent mechanism which represents the stiffness model of the 3-UPU TPM are used. The second index is the clearance index which corresponds to the maximum position errors of the platform due to a given clearance in the revolute joints. First, the analytic expression of the pose error of the platform due to the clearance in the revolute joints is presented which depends on the value of the external wrench applied to the platform. Then, a numerical method based on a MATLAB function is proposed to compute the maximum position errors of the platform.

This work is organized as follows. Chapter 1 presents the potential of the 3-UPU topology by proposing six new architectures and showing the influence of both the direction of the revolute joint axes on the base and on the platform respectively and the leg position, on the shape of the singularity loci of the manipulator. In Chapter 2, a procedure to select the best architecture of the 3-UPU TPM for a given task is presented. This procedure is based on some performance indexes. Chapters 3 presents the stiffness of the 3-UPU TPM and the position of the platform due to the clearance in the revolute joints by means of two indexes which, conversely will be used to apply the procedure presented in Chapter 2. A case study is presented which shows the efficiency of the proposed selection procedure. Finally, some concluding remarks will be presented.

Chapter 1: The potential of the 3-UPU TPM

The influence of both the directions of the base/platform revolute axes and the leg position is further investigated and six new architectures of the mechanism which exhibit interesting performances are presented in this Chapter.
Moreover, for the architectures where the three legs of the manipulator might intersect at one point, some manufacturing solutions are proposed for the leg collision avoidance.

1.1. Background on the 3-UPU TPM

A schematic of the 3-UPU TPM is shown in Fig. 1.1. The prismatic joints are actuated. Each universal joint comprises two revolute pairs with intersecting and perpendicular axes, centred at point B_i, i = 1,2,3 in the base and at point A_i, i = 1,2,3, in the platform.
The platform pure translational motion is obtained (platform rotation is totally prevented) when the following geometric conditions are satisfied for each leg [4,6,9]:
- the axes of the two intermediate revolute pairs (defined by the unit vectors $\mathbf{q}_{2i}$, i = 1,2,3 and $\mathbf{q}_{3i}$, i = 1,2,3) are parallel to each other;
- the axes of the two ending revolute pairs (defined by the unit vectors $\mathbf{q}_{1i}$, i = 1,2,3 and $\mathbf{q}_{4i}$, i = 1,2,3) are parallel to each other.
What follows in this section refers to a special family of 3-UPU TPM architecture: the one that has the three axes of the revolute pairs in the base/platform in a same plane respectively.

The singularity of the manipulator, i.e., when the relationship between the external wrench applied on the platform and the forces and moments applied on each leg, that are related by the Jacobian matrix **J** is no longer a one-to-one relationship, occurs when the determinant K of the Jacobian matrix, K = det**J**, vanishes. This condition is given by [9]:

$$\left[\mathbf{s}_1.\left(\mathbf{s}_2\times\mathbf{s}_3\right)\right].\left[\mathbf{u}_1.\left(\mathbf{u}_2\times\mathbf{u}_3\right)\right]=0 \tag{1.1}$$

where $\mathbf{s}_i$, $\mathbf{u}_i$, i = 1,2,3, (Fig. 1.1) are respectively the unit vector of the i-th leg A_iB_i and the unit vector orthogonal to the cross link of the universal joint connecting the i-th leg to the base/platform.

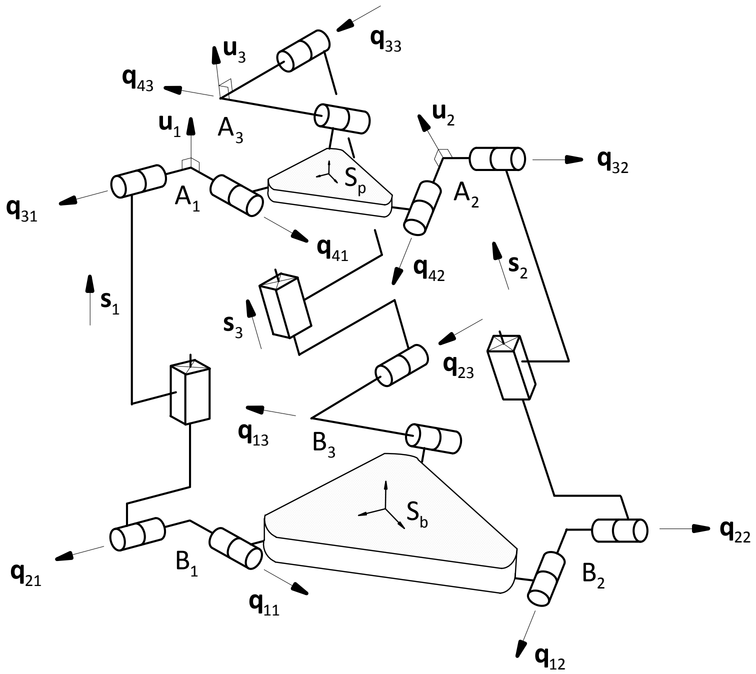

Figure 1.1. *The 3-UPU Translational Parallel Manipulator*

Equation (1.1) can be satisfied when:
i) all unit vectors $\mathbf{s}_i$, i = 1,2,3, become mutually parallel or coplanar [6,14];
ii) two out of three vectors $\mathbf{u}_i$, i = 1,2,3, are parallel. By geometric inspection, it can be seen that this condition occurs when two axes of the revolute pairs of the platform ($\mathbf{q}_{4i}$, $\mathbf{q}_{4j}$, i=1,2; j=2,3; i≠j) projects on the two corresponding axes of the base ($\mathbf{q}_{1i}$, $\mathbf{q}_{1j}$), providing the projection direction is along the shortest distance of the two axes.
Condition ii) is a concise and geometric definition of singularity occurrence and it represents a powerful geometric tool for detecting this type of singularity.

In [23,24], two architectures of the 3-UPU TPM have been defined. They are here recalled for completeness of presentation.
The first one, defined as architecture 1.A and shown in Fig. 1.2, occurs when the axes $\mathbf{q}_{1i}$, i = 1,2,3 and $\mathbf{q}_{4i}$, i = 1,2,3 of the revolute pairs in the base/platform two-by-two intersect at three points (points C_i, i = 1,2,3, at the base which define a plane π shown in Fig. 1.2).

In Fig. 1.2 only the revolute pairs on the base and on the platform are represented for clarity, all other ones are omitted. The same simplification has been adopted for all the next figures of this Chapter.

A system of reference S_b fixed to the base with origin O_b (the centre of the circle with radius b defined by the centers of the universal joint connected to the base B_i, i = 1,2,3) is chosen. Axes x and y are on the plane π, with x axis through point B_1, z axis is pointing from the base to the platform, while y axis is taken according to the right hand rule.

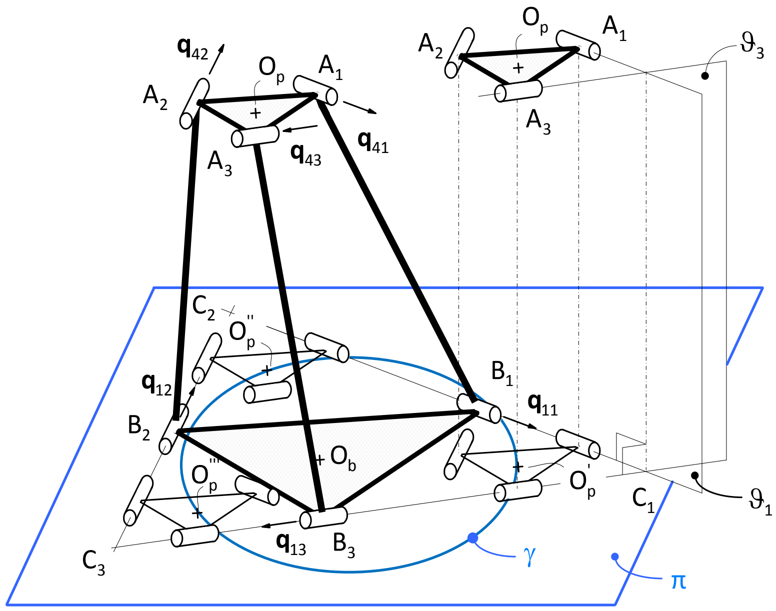

Figure 1.2. *Singularity loci for the architecture 1.A of the 3-UPU TPM*

According to the singularity condition defined above, the singularity for the architecture 1.A occurs when:

- the reference point of the platform O_p (center of the circle with radius p defined by the centers of the universal joint connected to the platform A_i, i = 1,2,3, and origin of the reference system S_p fixed to the platform with x axis through point A_1 and z axis is pointing upward from the base to the platform, while y axis obtained according to the right hand rule) lies on the plane π. This plane corresponds to z = 0;
- points A_i and A_j (i = 1,2,3, j = 1,2,3, i ≠ j) belong respectively to the two planes ϑ_i and ϑ_j orthogonal to the plane π and containing respectively $\mathbf{q}_{1i}$ and $\mathbf{q}_{1j}$ (which are the unit vectors of the revolute pairs joining the base to the i-th and the j-th leg respectively). In this position also $\mathbf{q}_{4i}$ and $\mathbf{q}_{4j}$, which are always parallel to $\mathbf{q}_{1i}$ and $\mathbf{q}_{1j}$, belong to the planes ϑ_i and ϑ_j. $\mathbf{q}_{4i}$ and $\mathbf{q}_{4j}$ are the unit vectors of the revolute pairs joining the platform to the i-th and the j-th leg respectively. This condition is represented in Fig. 1.2 when point O_p of the platform projects into point O_p' in the plane π. Similar conditions occur considering vectors $\mathbf{q}_{41}$ and $\mathbf{q}_{42}$, and vectors $\mathbf{q}_{42}$ and $\mathbf{q}_{43}$, which lead to define similar points O_p'' and O_p''' in the plane π. Analytically, it can be proved that a singularity locus is a right cylinder Υ [6], with circular directrix γ and axis coincident with the z axis of S_b. Therefore, conversely, once defined the points O_p', O_p'' and O_p''', the circle γ is defined and the cylinder Υ is defined too. The three points can be easily found by geometrical inspections thus representing a simple and efficient method to easily find the cylinder Υ. This cylinder has radius r = 2(b-p).

- the base and the platform have the same size (all unit vectors $\mathbf{s}_i$, i = 1,2,3, become mutually parallel for any position of the platform). The manipulator is in singular position and the manipulator is structurally singular [6,9,14].

The second architecture (defined as architecture 1.B) is obtained by disconnecting the platform of the architecture 1.A from the legs and rotating it 180 degrees about the z axis of S_b which is defined as in the previous 3-UPU TPM architecture, then connecting again the legs to the same corresponding platform revolute pairs. This makes the three legs intersect at one point as shown in Fig. 1.3. This is a practical drawback. However, manufacturing solutions can overcome it. Indeed, three efficient manufacturing solutions will be present in the next section to avoid the collision of the legs [23].
The singularity loci of this architecture correspond respectively to:
- the plane π (z = 0);
- the cylinder with axis z of S_b and with radius r = 2(b+p);
- architecture singularity (when the base and the platform have the same size).

It is worth noting that, for the same size of the base and the platform for the two architectures defined above, the 3-UPU TPM with architecture 1.B has a larger cylinder of singularity than that with architecture 1.A, and it allows a larger workspace free from singularity inside the cylinder.

1.2. New architectures of the 3-UPU TPM

This section presents new architectures of the 3-UPU TPM. 3-UPU TPMs that can be classified in two main families: 3-UPU TPM with coplanar base/platform revolute joints axes and with skew base/platform revolute joints axes: named as planar and skew architectures for brevity.
Planar architectures have the three revolute joint axes connecting the base/platform with the leg on a plane (for the base, plane π in Fig. 1.2), while the skew architectures have these three axes not belonging to a same plane but they are skewed.

1.2.1. Planar architectures

In this section, two new architectures of the 3-UPU TPM are presented. The first architecture (defined as architecture 2.A) is obtained by taking two axes of the base/platform revolute pairs out of the three mutual parallel. Fig. 1.4 shows a case with the unit vectors $\mathbf{q}_{11}$ and $\mathbf{q}_{13}$ mutually parallel and orthogonal to the unit vector $\mathbf{q}_{12}$ of the third axis. The centers of the universal joints in the base/platform are chosen so as to have the angle between the vectors O_bB_i and O_bB_{i+1}, i = 1,2,3, respectively the vectors O_pA_i and O_pA_{i+1}, i = 1,2,3, equal to 2π/3. S_b is defined as in the previous architectures.
Singularity loci: similarly to the two previous architectures (architectures 1.A and 1.B) also this new architecture 2.A when b = p is structurally singular.

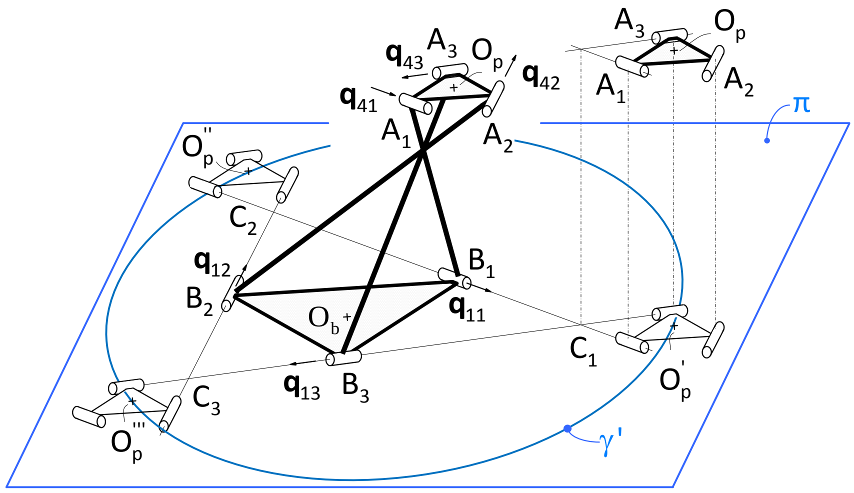

Figure 1.3. *Singularity loci for the architecture 1.B of the 3-UPU TPM*

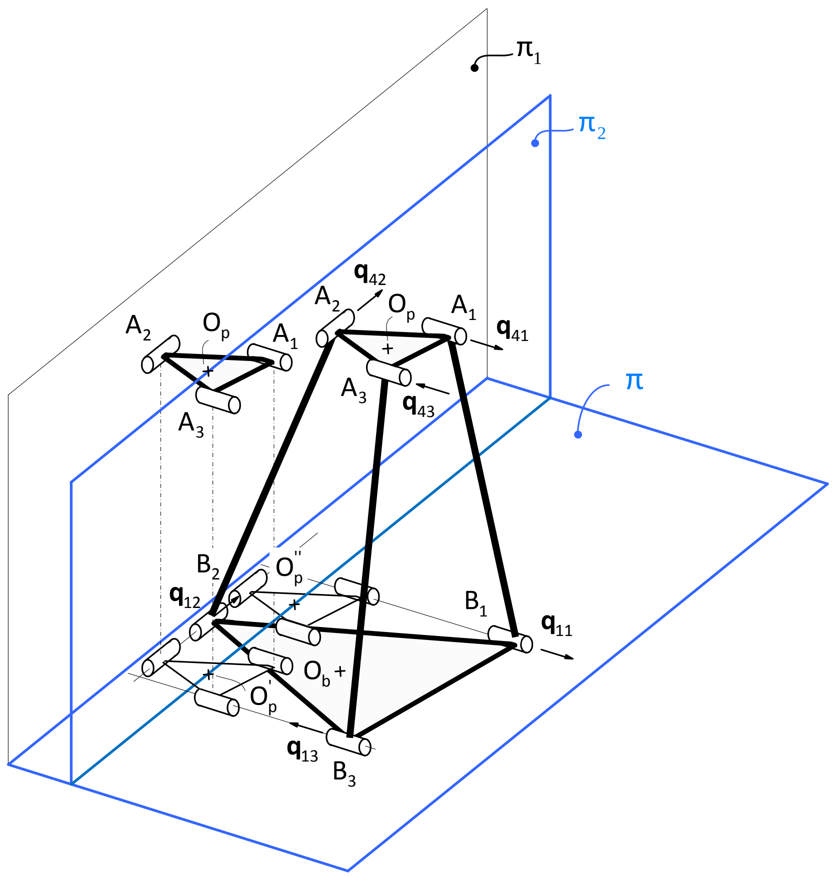

Figure 1.4. *Singularity loci for the architecture 2.A of the 3-UPU TPM*

For b ≠ p, Eqn. (1.1) is satisfied when: the unit vectors $\mathbf{s}_i$, i = 1,2,3, become coplanar and belong to the plane π (z = 0), and two out of three unit vectors $\mathbf{u}_i$, i = 1,2,3, become parallel. This latter condition occurs when A_i and A_j, i = 1,2,3, j = 1,2,3, i≠j, belong respectively to the two planes orthogonal to the plane π and containing respectively $\mathbf{q}_{1i}$

and $\mathbf{q}_{1j}$ (defined as in the previous 3-UPU TPM architectures). This condition is shown in Fig. 1.4 for the position of the platform when point O_p projects into point O_p'. A similar position occurs when point O_p projects into O_p''. The third point, analogous to O_p''' of the previous architectures goes to infinite since $\mathbf{q}_{13}$ and $\mathbf{q}_{11}$ are parallel. Therefore, the circle γ', directrix of the singularity cylinder ϒ', becomes a line passing through points O_p' and O_p''. As a consequence, the singularity cylinder becomes the plane π_2, orthogonal to the plane π and passing through the two points O_p' and O_p''.
The equation of this plane (π_2) can be determined analytically as follows:

$$y = \frac{\lambda_{12}}{\kappa_{12}}\left(x-(b-p)\cos\left(\frac{2\pi}{3}\right)\right)+(b-p)\sin\left(\frac{2\pi}{3}\right) \qquad \forall z \in \mathbb{R} \tag{1.2}$$

where κ_{12} and λ_{12} are respectively the x and y components of the unit vector $\mathbf{q}_{12}$ in the reference system S_b, and x, y and z are the coordinates of the reference point O_p of the platform in the system S_b.

Let α be the angle between the axes of the two revolute pairs connecting the first and the third leg to the base, i.e. the angle between the unit vectors $\mathbf{q}_{11}$ and $\mathbf{q}_{13}$, $\alpha = \left(\mathbf{q}_{11}, \mathbf{q}_{13}\right)$. In Fig. 1.5 that reports the intersection of the singularity loci with the plane π (x,y plane of S_b) for different values of the angle α, shows the changing of the singularity loci from a cylinder to a plane according to the value of the angle α, i.e, when the value

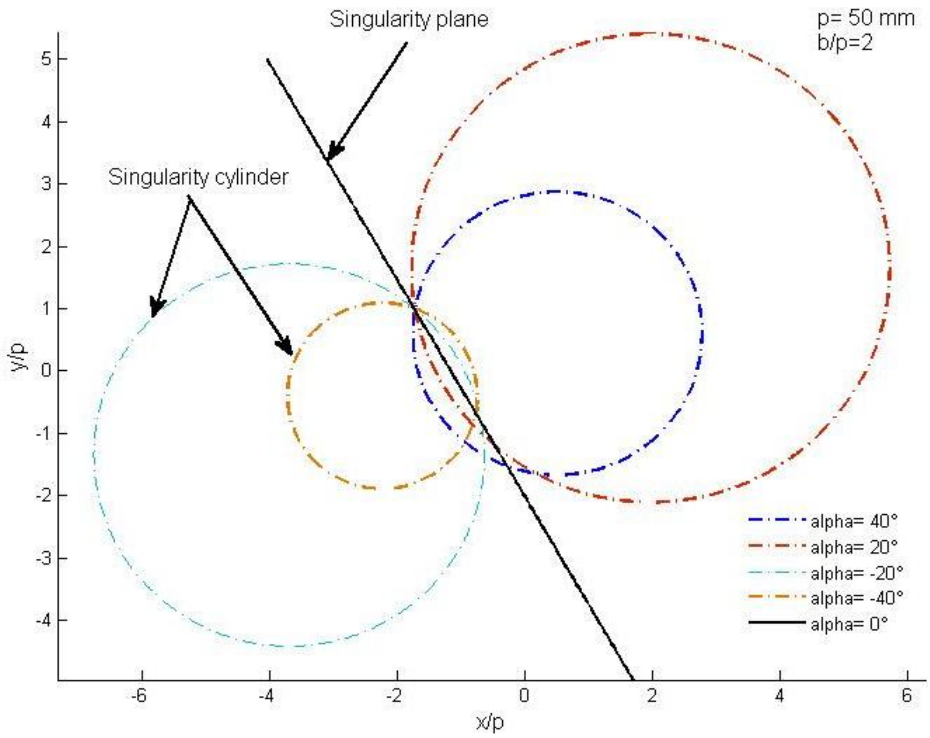

Figure 1.5. *Singularity cylinder and singularity plane of the 3-UPU TPM*

of the angle α is equal to zero or 180 degrees, the singularity loci correspond to a plane. If this condition does not occurs, the singularity loci correspond to a cylinder.
It is worth noting that 3-UPU TPM with architecture 2.A have a workspace consisting of a volume, plane π_2 apart, free from singularity.

Similarly to what done for the transition from architecture 1.A to the architecture 1.B (changing the location of the legs), a further 3-UPU TPM architecture can be devised. Indeed, by disconnecting the platform from the legs, rotating it 180 degrees about z axis of S_b (defined as in the previous 3-UPU TPM architectures), then reassembling it to the same corresponding platform revolute pairs, still keeping the same direction of the base revolute pairs, a new architecture defined as architecture 2.B, can be found as shown in Fig. 1.6. This architecture leads to the intersection of the three legs at one point.
By the same procedure as in the previous cases, the singularity loci of this architecture are found and it corresponds to two planes, π and π'_2.
The equation of π'_2 can be determined analytically as follows:

$$y = \frac{\lambda_{12}}{\kappa_{12}}\left(x - (b+p)\cos\left(\frac{2\pi}{3}\right)\right) + (b+p)\sin\left(\frac{2\pi}{3}\right) \qquad \forall z \in \mathbb{R} \tag{1.3}$$

where κ_{12} and λ_{12} are respectively the x and y components of the unit vector $\mathbf{q}_{12}$ in the reference system S_b.
Similarly to the previous case (architecture 2.A), it is worth noting that 3-UPU TPM with architecture 2.B have a workspace consisting of a volume, plane π'_2 apart, free from singularity.

1.2.2. Skew architectures

By considering a skew relative position of the axes of the base/platform revolute joints, new architectures were found and presented in [23]. Their schematics are reported in Fig. 1.7-1.10. In this section, a complete study on the singularity loci is presented. For the first architecture defined as architecture 3.A, the axes of two revolute pairs on the base are on the plane π (z = 0). The axis of the third revolute pair is orthogonal to the plane π as shown in Fig. 1.7-a. The singularity loci correspond to [23]:
- the plane π.
- the structural singularity, i.e., the base and the platform have the same size.
- three lines δ_{ij}, i = 1,2; j = 2,3; i ≠ j, which represent the locus of the reference point O_p of the platform when, according to the method reported at section 1.1, two axes of the revolute pairs of the platform ($\mathbf{q}_{4i}$, $\mathbf{q}_{4j}$) projects on the two corresponding axes of the base ($\mathbf{q}_{1i}$, $\mathbf{q}_{1j}$) providing the projection direction is along the unit vector $\mathbf{v}_{ij}$, i = 1,2; j = 2,3; i ≠ j, of the shortest distance among the two axes. A geometrical inspection shows that the

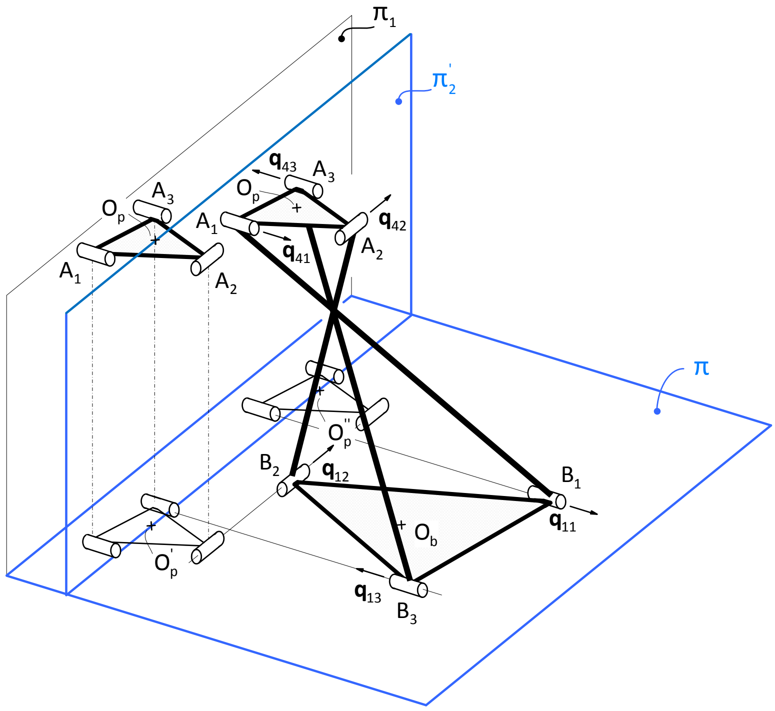

Figure 1.6. *Singularity loci for the architecture 2.B of the 3-UPU TPM*

lines δ_{23} and δ_{13} are on the plane π. While the line δ_{12} is orthogonal to the plane π.
In [23] only some information on the singularities were reported based on geometric influences, then a complete study is reported based also on analytical (development) tools. By substituting the expression of the vectors $\mathbf{s}_i$ and $\mathbf{u}_i$, i = 1,2,3, in Eqn. (1.1) and equating the numerator to zero, it is possible to find:

$$z\left(Ax^2 + Bxy - Ay^2 + Dx + Ey + F\right) = 0 \tag{1.4}$$

where x, y and z are the coordinates of the reference point O_p of the platform in the system S_b and the coefficients A, B, D, E and F depend on the x and y coordinates of the point O_p in the system S_b, on the direction of the revolute joint of the base and on the radii b, p (full expression of the coefficients A, B, D, E and F are reported in Appendix A).
Equation (1.4) is satisfied when:

$$\begin{cases} z = 0 \\ Ax^2 + Bxy - Ay^2 + Dx + Ey + F = 0 \quad \forall z \in \mathbb{R} \end{cases} \tag{1.5}$$

Thus, the singularity loci correspond to the plane π (z = 0) and from the second equation of Eqn. (1.5), to two surfaces Γ_1 and Γ_2 which are ruled surfaces (represented in Fig. 1.7-a)

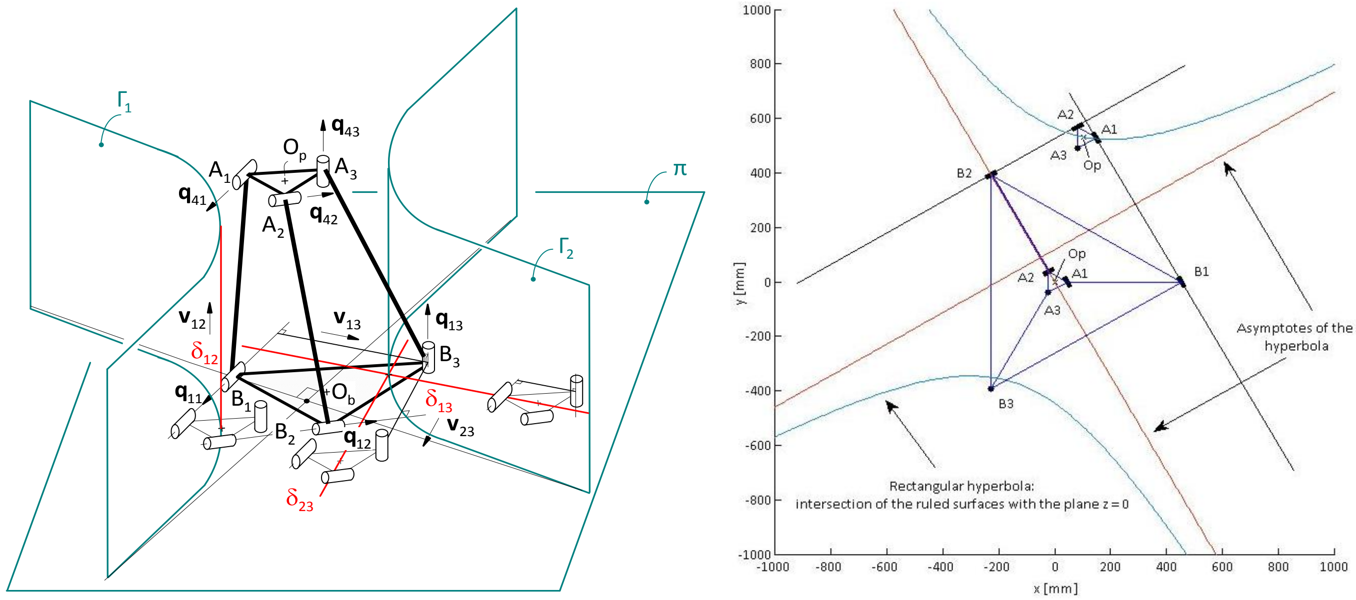

(a) *(b)*

Figure 1.7. *(a) Singularity loci for the architecture 3.A of the 3-UPU TPM*
(b) View from the top of the singularity loci for the architecture 3.A of the 3-UPU TPM

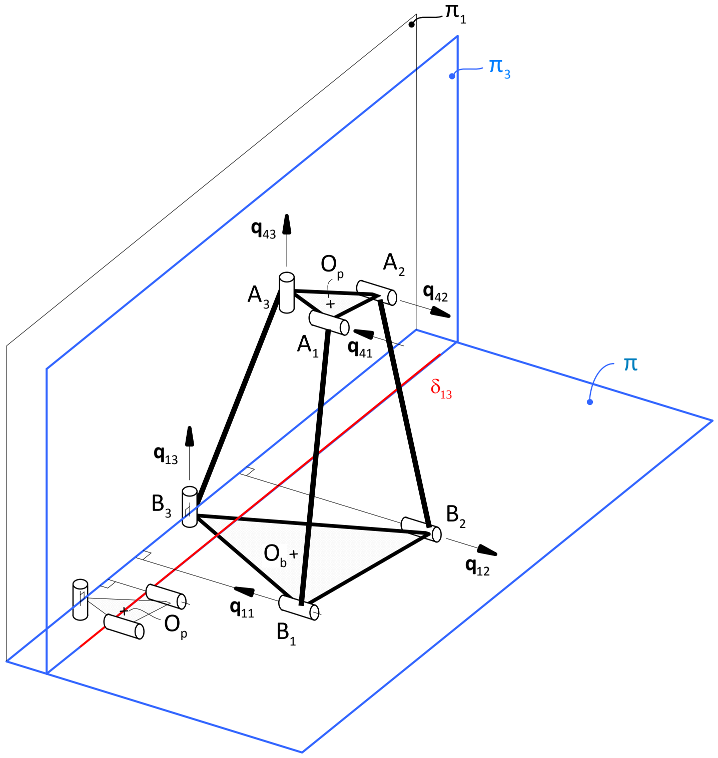

Figure 1.8. *Singularity loci for the architecture 4.A of the 3-UPU TPM*

that intersect the plane π on a rectangular hyperbola as shown in Fig. 1.7-b.
For the second architecture, defined as architecture 4.A, two axes of the revolute pairs on

the base are mutually parallel and belong to the plane π, while the third one is orthogonal to the plane π as shown in Fig. 1.8. The singularity loci correspond to the plane π and to a line δ_{13} (δ_{23}) (locus of the platform reference point O_p) on this plane obtained by the projection of the axes of the two revolute pairs $\mathbf{q}_{11}$ and $\mathbf{q}_{13}$ ($\mathbf{q}_{12}$ and $\mathbf{q}_{13}$) of the platform on the two corresponding axes of the base in the direction orthogonal to these two axes. It can be concluded that the singularity loci is the plane π [23].

Like the previous architecture, by substituting the expression the unit vectors $\mathbf{s}_i$ and $\mathbf{u}_i$, i = 1,2,3, in Eqn. (1.1) and equating the numerator to zero, an equation similar to Eqn. (1.4) is obtained, but in this case, the coefficients A and B are equal to zero, therefore Eqn. (1.4) becomes:

$$z(Dx + Ey + F) = 0 \tag{1.6}$$

Thus, the singularity loci correspond to two planes: the plane π (z = 0) and the plane π_3 (orthogonal to π and containing the line δ_{13} (δ_{23}) as shown in Fig. 1.8) which has the following equation:

$$y = -\frac{(Dx + F)}{E} \qquad \forall z \in \mathbb{R} \tag{1.7}$$

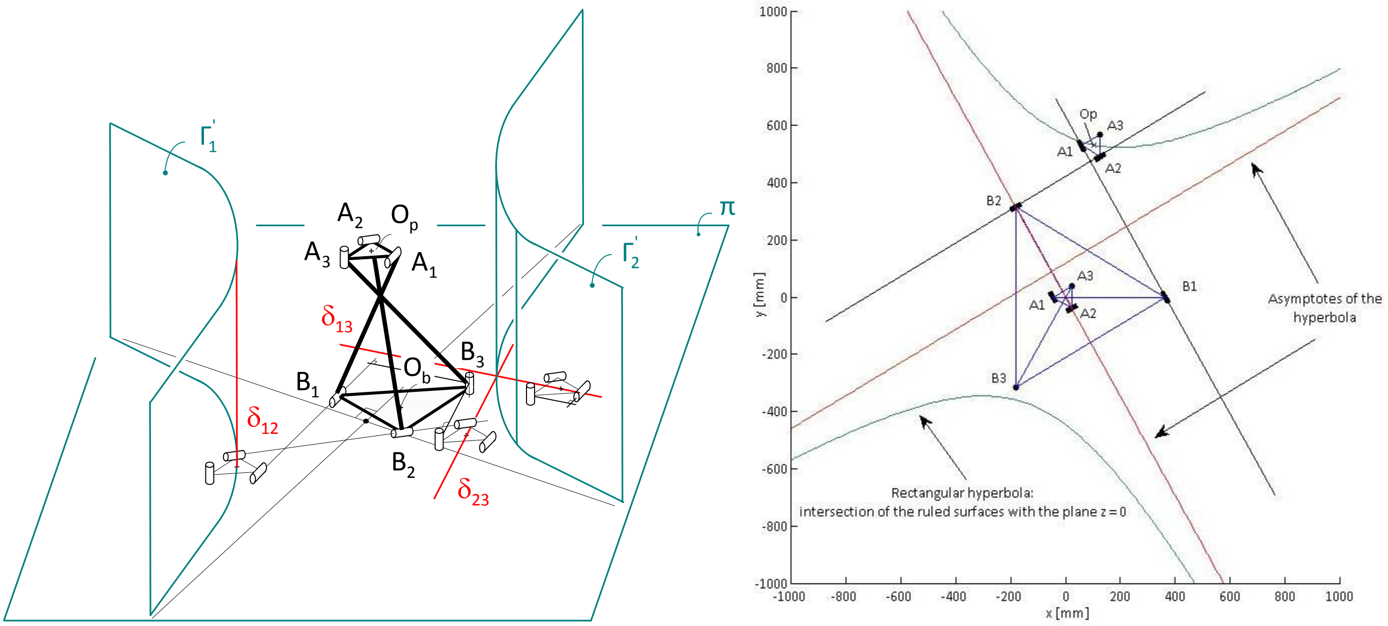

(a) *(b)*

Figure 1.9. *(a) Singularity loci for the architecture 3.B of the 3-UPU TPM*
(b) View from the top of the singularity loci for the architecture 3.B of the 3-UPU TPM

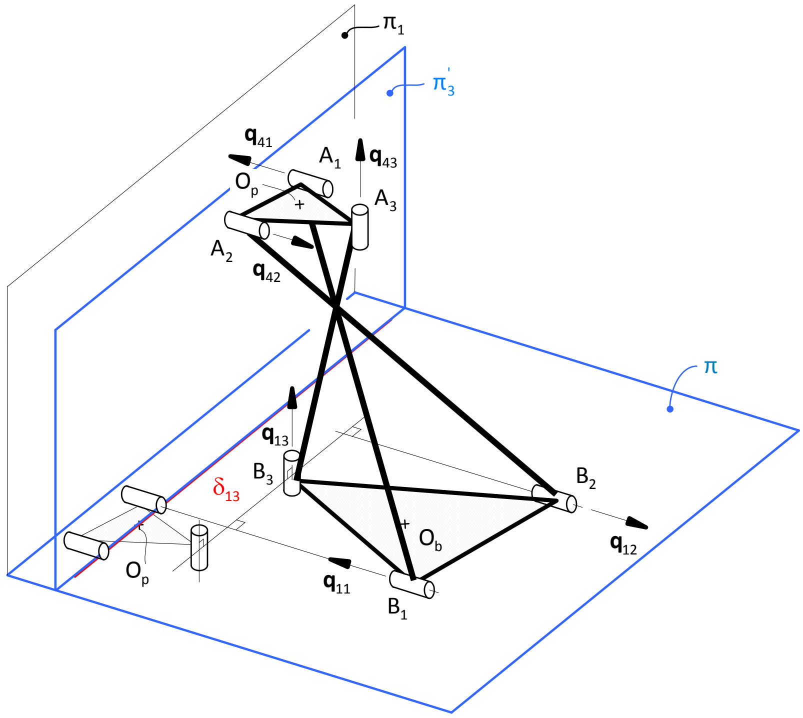

Figure 1.10. *Singularity loci for the architecture 4.B of the 3-UPU TPM*

Similarly to what done for the transition from architecture 1.A to the architecture 1.B (changing the location of the legs), a further 3-UPU TPM architectures can be devised. Indeed, by disconnecting the platform from the legs of the architectures 3.A and 4.A respectively, rotating it 180 degrees about z axis of S_b, then reassembling it to the same corresponding platform revolute pairs, still keeping the same direction of the base revolute pairs, two new architectures defined as architecture 3.B and architecture 4.B, can be found as shown in Fig. 1.9-a,b and Fig. 1.10. These architectures lead to the intersection of the three legs at one point. Analogously to the architectures 3.A and 4.A, the singularity loci of the architecture 3.B is the plane π and two ruled surfaces Γ_1' and Γ_2', and for the architecture 4.B, the two planes π and π_3'.

1.3. Manufacturing solutions for the leg collision avoidance of the 3-UPU TPM

In this section, three manufacturing solutions are presented in order to avoid the leg collision in the architectures of type B (crossed legs) of the 3-UPU TPM. Architecture 1.B is taken (for clarity) as an example of this type of 3-UPU TPM [23].

The first manufacturing solution, is to rebuilt the platform of the manipulator. This is obtained by disconnecting the platform of this architecture from the legs and rotating it by a suitable angle β about the z axis of S_b, then connecting again the legs to the platform still keeping the same base revolute joint axes. This means to manufacture a platform with the revolute axis directions rotated of β (clockwise in the example shown in Fig. 1.11-a) with respect to the architecture 1.B. This makes it possible to avoid the leg collision.

In Fig. 1.11-a, the universal joints on the base and on the platform are represented by points for clarity, and the prismatic ones are omitted.

After manufacturing the new platform, the coordinates of the center of the universal joint that connect the i-th leg to the platform A'_i, i = 1,2,3, are given by:

$$\begin{cases} \overrightarrow{O_pA_i^{'}} = \cos\beta\,\overrightarrow{O_pA_i} + \sin\beta\,\overrightarrow{O_pA_i^{''}} \\ \overrightarrow{O_pA_i^{''}} \perp \overrightarrow{O_pA_i} \\ \left\|\overrightarrow{O_pA_i^{''}}\right\| = \left\|\overrightarrow{O_pA_i}\right\| \end{cases} \qquad i=1,2,3 \tag{1.8}$$

where A_i, i = 1,2,3, are the centers of the universal joints in the platform of the architecture 1.B.

The second manufacturing solution, schematically shown in Fig. 1.11-b, is to rebuilt both the base and the platform of the architecture 1.B in order to have the coordinates of the centers of universal joints at the base and at the platform, respectively B'_i and A'_i, i = 1,2,3, (see Fig. 1.11-b), given as follows:

$$\begin{cases} \overrightarrow{O_bB_i^{'}} = \overrightarrow{O_bB_i} + e\,\mathbf{q}_{1i} \\ \overrightarrow{O_pA_i^{'}} = \overrightarrow{O_pA_i} + e\,\mathbf{q}_{4i} \end{cases} \qquad i=1,2,3 \tag{1.9}$$

where B_i and A_i, i = 1,2,3, are respectively the center of the universal joints in the base and in the platform of the original architecture 1.B; $\mathbf{q}_{1i}$ and $\mathbf{q}_{4i}$, i = 1,2,3, are respectively the unit vectors of the revolute joints on the base and on the platform, which maintain the same directions of the original architecture 1.B; e is a given distance (offset) between the corresponding center of universal joints in the platform of the architecture 1.B and the platform rebuilt.

The third manufacturing solution, schematically shown in Fig. 1.11-c, is to rebuilt the second and the third link of each leg of the architecture 1.B in order to change the physical position of the prismatic pairs on each leg along the vector $\overrightarrow{E_iF_i}$, where the coordinate of the points E_i and F_i, i = 1,2,3 are given by:

$$\begin{cases} \overrightarrow{O_bE_i} = \overrightarrow{O_bB_i} + d\,\mathbf{q}_{2i} \\ \overrightarrow{O_pF_i} = \overrightarrow{O_pA_i} + d\,\mathbf{q}_{3i} \end{cases} \qquad i=1,2,3 \tag{1.10}$$

where B_i and A_i, i = 1,2,3, are respectively the centers of the universal joints in the base and in the platform of the architecture 1.B; $\mathbf{q}_{2i}$ and $\mathbf{q}_{3i}$, i = 1,2,3, are respectively the unit vectors of the intermediate revolute joints of the i-th leg; d is a given distance between the directions of the prismatic pairs for the architecture 1.B and the manipulator architecture after rebuilding.

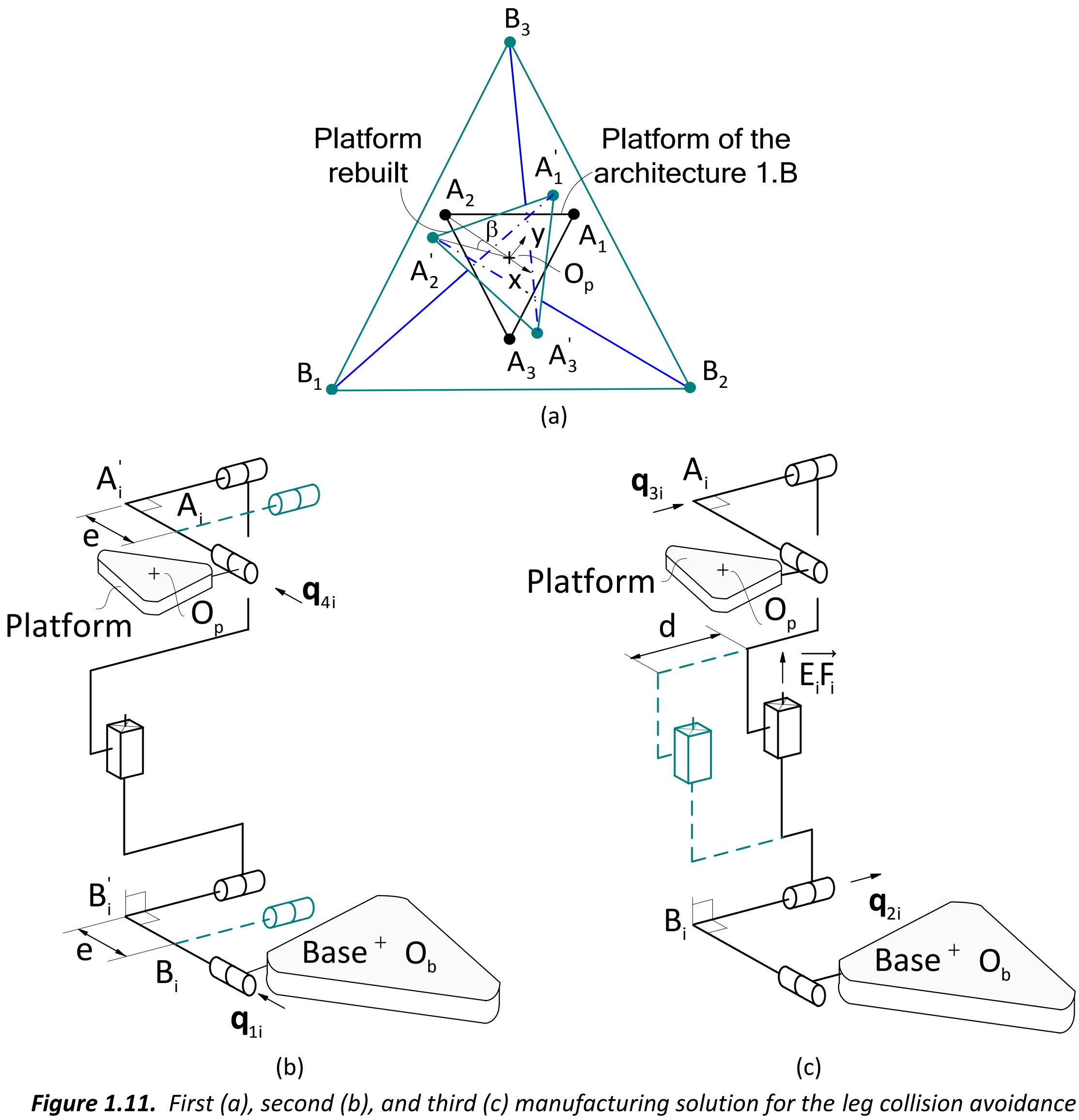

Figure 1.11. *First (a), second (b), and third (c) manufacturing solution for the leg collision avoidance of the architecture 1.B*

Chapter 2: Procedure to select the best architecture of the 3-UPU TPM for a given task

In this chapter, a procedure to select the best 3-UPU TPMs architecture among the eight ones (1.A, 1.B, 2.A, 2.B, 3.A, 3.B, 4.A and 4.B) reported in Chapter 1 for a given task, is presented. A complementary task is, in particular, to have a given Cartesian workspace of the platform free from singularities. It is worth noting that the proposed procedure can be applied (in general) to any 3 DOF manipulators.

The core of the procedure is the definition of a number of geometrical indexes which will be used to select the best architecture of the manipulator according to the given task. This procedure is composed of five main steps.

Before proceeding to the first step, a security index related to the singularity occurrence of the manipulator should be define. Since K, which represents the determinant of the Jacobian matrix **J** (provides a relation between the external wrench applied at the reference point O_p of the platform and the forces and moments applied on each leg), is a vector product of unit vectors:

$$K = \left[\mathbf{s}_1.\left(\mathbf{s}_2 \times \mathbf{s}_3\right)\right].\left[\mathbf{u}_1.\left(\mathbf{u}_2 \times \mathbf{u}_3\right)\right] \tag{2.1}$$

the value of K ranges from -1 to 1, K being equal to zero at singularity. The given value of K, K_d can be used as a security index which represents how far the manipulator is from a singularity configuration. K depends on the rate b/p (b and p are respectively the radius of the circles defined by the centers of the universal joints connected to the base, B_i, i = 1,2,3, and the centers of the universal joints connected to the platform, A_i, i = 1,2,3) and on the position of the reference point O_p of the platform in the workspace. With reference to Eqn. (2.1), det**J** = K_d represents a closed surface in the Cartesian space inside/outside of which K is smaller/greater than a given value of K, K_d [6,16].

The first step corresponds to the following:

- given the manipulator workspace W_d chose to locate it above the plane π (z = 0) defined in Chapter 1.

- define the same desired value K_d of the security index for the different architectures of the 3-UPU TPM presented in Chapter 1 according to the task that the manipulator has to perform (the value of K_d is between 0 and 1);
- chose a value for p (radius of the circle that belongs the centers of the universal joints A_i, i = 1,2,3 connected to the platform) as smaller as possible according to the manufacturing costs and the strength of materials used;
- find the smallest sphere S that contains the given workspace W_d, let d_S be its diameter;
- the sphere S must be inside and tangent to the closed surface $K = K_d$. Indeed, for the chosen p, many solutions can be found, each of them is characterized by a different value of the rate b/p. Different cases may arise: the sphere S can be tangent to the surface $K = K_d$ in different positions as shown in Fig. 2.1.
- the rate b/p which corresponds to the smallest surface $K = K_d$ that contains the sphere S (and is also tangent to the sphere S) is chosen, as shown in Fig. 2.1-a.

The second step is the definition of an objective function that the manipulator has to satisfy. The objective function can be defined by a proper weighted selection of one or more indexes (will propose in the next Chapter), each of them is related to a specific property of the manipulator, such as size, singularity, stiffness and accuracy (corresponds to the maximization of the platform position error due to the clearance in revolute joints of the 3-UPU TPM) of the manipulator.

The third step is to compute the selected indexes for a section W of the given workspace. The computation should have to be performed on the whole workspace. However, this is a time consuming step that is not worth in most cases, thus, quite often, it can be avoided by limiting the computation to a significant subset of the workspace, for instance, a chosen section of it. The chosen section W contains the center C_S of the sphere S and is parallel to the plane π (z = 0).

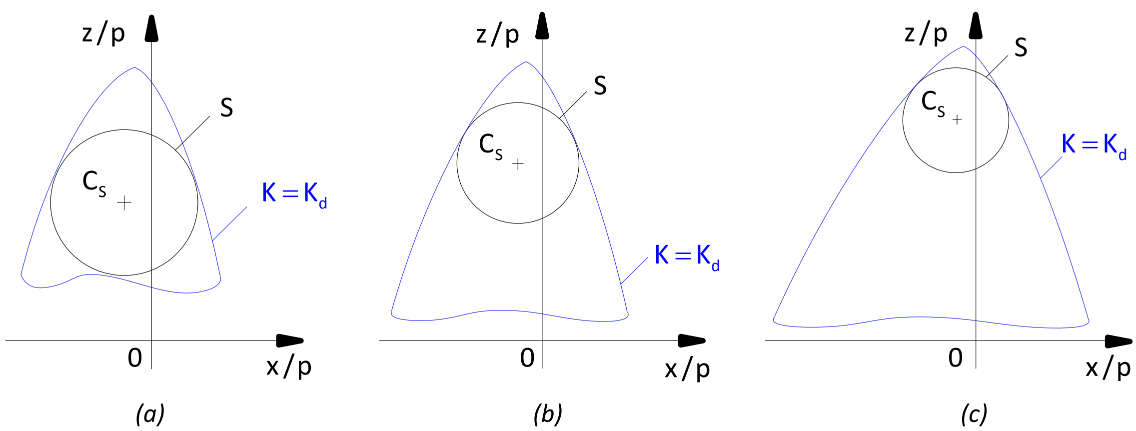

Figure 2.1. *Three cases of tangency between the sphere S and the closed surface K=K_d*

The fourth step is to normalize the selected indexes computed in the previous step, in order to find a criterion of comparison, as follows:

$$T_i = \frac{\int_W t_i . dW}{\int_W dW} \qquad i = 1,..,n \tag{2.2}$$

where t_i and n are respectively the i-th index value and the number of indexes, W is the selected subset of the workspace and T_i is the normalized i-th index value.
There is no closed-form solution for Eqn. (2.2), then the integral of the i-th index, is calculated numerically, which can be approximated by a discrete sum:

$$T_i \approx \frac{1}{N_v} \sum_{v \in W} t_i \qquad i = 1,...,n \tag{2.3}$$

where v is one of N_v points which are uniformly distributed in the section W of the given workspace.
The previous four steps have to be completed for all the available investigated architectures.

The fifth step is to select the 3-UPU TPMs architecture which best satisfies the selected objective function (see second step above).

Chapter 3: Indexes proposed

In this chapter, two indexes are proposed in order to select the best 3-UPU TPMs architecture among the eight architectures of the 3-UPU TPM presented in Chapter 1 by applying the procedure detailed in Chapter 2. These indexes correspond respectively to the stiffness of the manipulator and to the maximum value of the platform position error due to the clearance in the revolute joints of the 3-UPU TPM. The indexes are called stiffness and clearance indexes respectively. The best architecture corresponds to the highest stiffness of the manipulator and the lowest position error of the platform due to the clearance in the revolute joints (highest accuracy of the manipulator).

3.1. Stiffness of the 3-UPU TPM

3.1.1. Stiffness matrix of the 3-UPU TPM

The focus of this section, is to present a stiffness index. In some cases, indeed, the deformation of the links under the applied loads must be taken into account. In this case, with the assumption of small deformations, the spatial force–deflection relation of the manipulator is linear, and is described by a 6x6 symmetric positive semi definite matrix called stiffness matrix **H**. i.e., this matrix provides the relation between the external wrench applied at the reference point of the platform and the displacement of the platform itself. According to the static analysis [12,16,22], when the external wrench is applied on the reference point of the platform of the 3-UPU TPM, the i-th leg is loaded by a torque m_{ti}, i = 1,2,3, by an axial forces f_i, i = 1,2,3, and a bending moment m_{bi}, i = 1,2,3. An upper bound of the variation of the rate bending moment/torque, μ_i, i = 1,2,3, applied on the i-th leg of the manipulator in the whole workspace is computed according to a procedure which will be detailed in the next section. The value of this upper bound is small than 0.5 when the axes of the revolute joints on the base and on the platform respectively are coplanar (this case corresponds to the planar architectures 1.A, 1.B, 2.A and 2.B of the manipulator). For this reason, the bending moment, m_{bi}, i = 1,2,3, will be neglected in the stiffness model of the i-th leg for the planar architectures of the manipulator. For the architectures when the base/platform revolute joints axes are skew (this case corresponds to the skew architectures 3.A, 3.B, 4.A and 4.B of the manipulator), it can be obtained that the bending moment m_{bi}, i = 1,2,3, applied on the i-th leg is still keeping the same direction when the reference point O_p of the platform moves in the whole workspace. According to this result, the legs can be rebuilt in order to support this bending moment m_{bi}, in the corresponding direction. Thus, the bending moment m_{bi}, i = 1,2,3, can be neglected in the stiffness model of the i-th leg for the skew architectures of the manipulator.

For a given input of the actuators, the 3-UPU TPM becomes a structure. Each leg can be considered as a serial chain of type UU, because the actuated prismatic pair variable is given.

Due to the torque m_{ti}, i = 1,2,3, and the axial force f_i, i = 1,2,3, the i-th leg undergoes a torsion and an axial deformation. Fig. 3.1 depicts the elastic model of the 3-UU structure, where k_{ri} and k_{ai}, i = 1,2,3, represent respectively the rotational and the axial stiffnesses of the i-th leg and the base and platform universal joints are not represented for simplicity (the platform, the base and the universal joints are considered as rigid, while the legs as deformable).

In order to consider the displacement of the platform produced by the deformation of the leg links due to the torque and to the axial force, additional elastic pairs are introduced for each of the i-th leg, namely: a revolute pair with the axis directed as the torque axis and a prismatic pair directed as the unit vector $\mathbf{s}_i$, i = 1,2,3, of the i-th leg, which can model respectively the torsional and the axial elastic deformation of the i-th leg, given by the variables θ^i_3 and d^i_4, i = 1,2,3, respectively as shown in Fig. 3.2. An equivalent manipulator is thus defined, as represented in Fig. 3.2, which allows a general

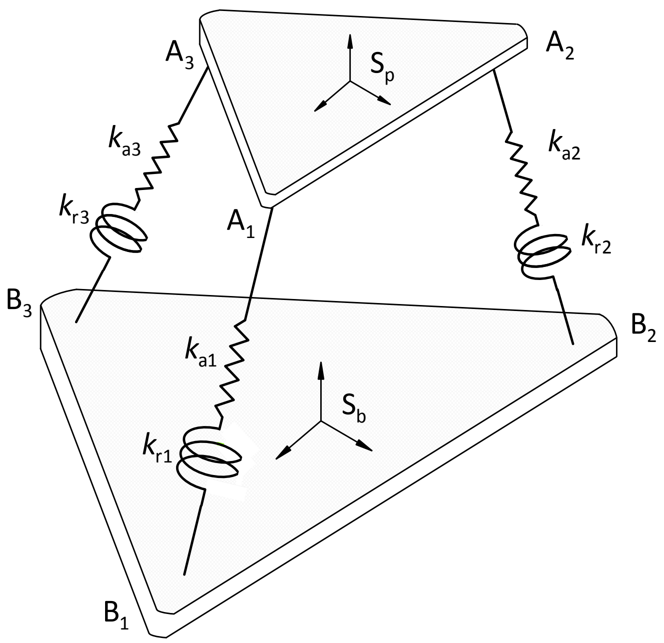

Figure 3.1. *Stiffness model of the 3-UPU TPM*

displacement of the platform (in 3D Cartesian space) that can be expressed as a function of the six variables θ^i_3 and d^i_4, i = 1,2,3. Therefore, the equivalent mechanism can model the influence on the platform displacement of the θ^i_3 and d^i_4 variables.

The stiffness matrix **H** that provides the relation between the external wrench, $[\mathbf{F}\ \mathbf{M}]^T$, applied at the reference point O_p of the platform and the displacement, $[\mathbf{t}\ \mathbf{r}]^T$, of the platform itself, is given by the following equation:

$$\begin{bmatrix} \mathbf{F} \\ \mathbf{M} \end{bmatrix} = \mathbf{H} \begin{bmatrix} \mathbf{t} \\ \mathbf{r} \end{bmatrix} \tag{3.1}$$

where **t** and **r** are respectively the displacement (translation and rotation) of the platform. **t** and **r** have to be intended as ‘small’ (infinitesimal) displacements.
The procedure to compute the stiffness matrix, **H**, is composed of five main steps.

The first one is to express the pose of the reference system S_p fixed to the platform with origin at point O_p with respect to system S_b fixed to the base (systems S_b and S_p are defined as in Chapter 1). In other word, to determine the 4x4 matrix, $\mathbf{N}^i$, i = 1,2,3, that transforms the homogenous coordinates of a point from S_p to S_b.
For the i-th leg, the 4x4 matrix $\mathbf{N}^i$, i = 1,2,3, (function of the joint variables θ^i_1, θ^i_2, θ^i_3, d^i_4, θ^i_5, θ^i_6 as shown in Fig. 3.2) which transforms the homogenous coordinates of a point from S_p to S_b corresponds to the product of the 4x4 matrices $\mathbf{C}^i_j$, i = 1,2,3; j = 1,..,6, that transform the homogenous coordinate of a point from the system S^i_j (attached to the link j-1 of the i-th leg) to the system S^i_{j+1} (attached to the link j of the i-th leg), j = 0,..,6, (S_0 and S_7 correspond respectively to S_b and S_p as shown in Fig. 3.2).
The systems S^i_j, i = 1,2,3; j = 1,..,6, are defined as follows:
The z-axis of S^i_j, is taken on the direction of the j-th revolute joint as shown in Fig. 3.2.
The x-axis of S^i_j is orthogonal to the two z axes of S^i_j and S^i_{j-1}.
The origin O^i_j of the system S^i_j, corresponds to the intersection between x and z axis. y axis is taken according to the right hand rule.
After the systems S^i_j, i = 1,2,3; j = 0,...,7, are defined, the Denavit Hartenberg parameters (θ^i_j, α^i_j, d^i_j, a^i_j) are determined and shown in Tab. 3.1 and Tab. 3.2 according to the architecture of the manipulator.
The variable a^i_j (θ^i_j) is the distance (angle) between the z axes of S^i_j and S^i_{j+1} along (about) x- axis of S^i_{j+1} and d^i_j (α^i_j) is the distance (angle) between the x axes of S^i_j and S^i_{j+1} along (about) x- axis of S^i_{j+1}. Thus, According to Fig. 3.2, Tab. 3.1 and Tab. 3.2, the matrices $\mathbf{C}^i_0,\ldots,\mathbf{C}^i_6$, i = 1,2,3, are determined by Denavit Hartenberg convention [25] and the matrix $\mathbf{N}^i$, i = 1,2,3, is computed by using the following equation:

$$\mathbf{N}^i\left(\theta^i_1, \theta^i_2, \theta^i_3, d^i_4, \theta^i_5, \theta^i_6\right) = \prod_{j=0}^{6} \mathbf{C}^i_j \qquad i=1,2,3 \tag{3.2}$$

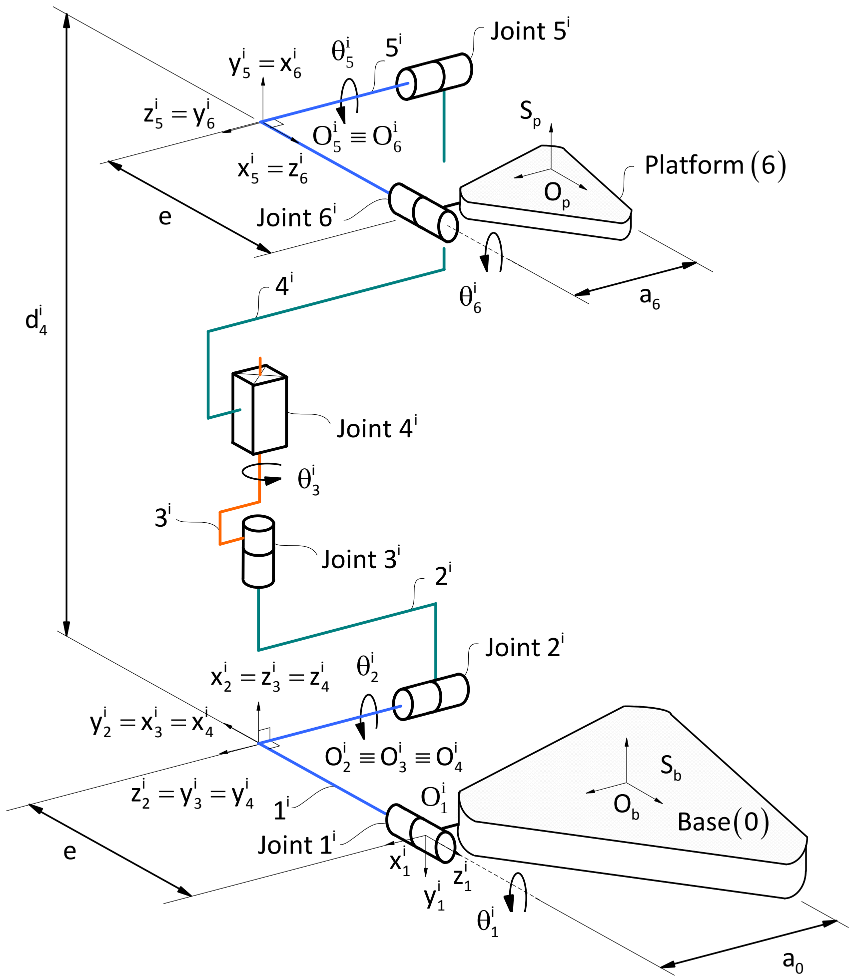

Figure 3.2. *Denavit Hartenberg Parameters on the i-th leg for the architectures of type A of the 3-UPU TPM*

Table 3.1. *Denavit Hartenberg parameters on the i-th leg for the architectures of type A of the 3-UPU TPM*

Link j^i	θ^i_j	α^i_j	d^i_j	a^i_j
Base (0)	0	$-\pi/2$	0	a_0
1^i	θ^i_1	$-\pi/2$	0	0
2^i	θ^i_2	$-\pi/2$	0	0
3^i	θ^i_3	0	0	0
4^i	0	$\pi/2$	d^i_4	0
5^i	θ^i_5	$\pi/2$	0	0
Platform (6)	θ^i_6	$\pi/2$	0	$-a_6$

Table 3.2. *Denavit Hartenberg parameters on the i-th leg for the architectures of type B of the 3-UPU TPM*

Link j^i	θ^i_j	α^i_j	d^i_j	a^i_j
Base (0)	0	$-\pi/2$	0	a_0
1^i	θ^i_1	$-\pi/2$	-e	0
2^i	θ^i_2	$-\pi/2$	0	0
3^i	θ^i_3	0	0	0
4^i	0	$\pi/2$	d^i_4	0
5^i	θ^i_5	$\pi/2$	0	0
Platform (6)	θ^i_6	$\pi/2$	e	$-a_6$

According to Eqn. (3.1), it can be concluded that the first column of the stiffness matrix **H** corresponds to the value of the vector (6x1) of the external wrench applied at the reference point O_p of the platform, when a platform translation of one unit along the x axis of the reference system S_b is performed.

Then, the second step is to find the variables θ_3^i and d_4^i, i = 1,2,3, which characterize respectively the torsion and the axial deformation of the i-th leg (i = 1,2,3) when a platform translation of one unit along the x axis of the reference system S_b is performed. In general, the homogeneous matrix **Σ** that transforms the homogenous coordinates of a point from S_b to S_p can be obtained by a successive rotations about axes non-fixed method and written as follows [26]:

$$\mathbf{\Sigma} = \begin{bmatrix} c\psi_2 c\psi_3 & -c\psi_2 s\psi_3 & s\psi_2 & x+\Delta x \\ s\psi_1 s\psi_2 c\psi_3 + c\psi_1 s\psi_3 & -s\psi_1 s\psi_2 s\psi_3 + c\psi_1 c\psi_3 & -s\psi_1 c\psi_2 & y+\Delta y \\ -c\psi_1 s\psi_2 c\psi_3 + s\psi_1 s\psi_3 & c\psi_1 s\psi_2 s\psi_3 + s\psi_1 c\psi_3 & c\psi_1 c\psi_2 & z+\Delta z \\ 0 & 0 & 0 & 1 \end{bmatrix} \tag{3.3}$$

where:

$$\psi_i = \gamma_i + \Delta\gamma_i \qquad i = 1,2,3 \tag{3.4}$$

and c(.) and s(.) stand for the cosine and the sine of the argument; γ_1, γ_2 and γ_3 are the Euler angle about x, y, and z axes respectively; Δx, Δy and Δz are respectively the small translations of the platform along x, y and z axes of S_b; $\Delta\gamma_1$, $\Delta\gamma_2$, $\Delta\gamma_3$ are respectively the small variation of the Euler angles.

Therefore $\mathbf{\Delta\delta} = (\Delta x, \Delta y, \Delta z, \Delta\gamma_1, \Delta\gamma_2, \Delta\gamma_3)^T$ represents a small variation of the displacement of the platform.

For a platform translation of one unit along the x axis of the reference system S_b, that is for $\mathbf{\Delta\delta} = (1,0,0,0,0,0)^T$, the variables θ_3^i and d_4^i, i = 1,2,3, in the i-th leg can be found by solving the following system:

$$\mathbf{N}^i = \mathbf{\Sigma}\,(\mathbf{\Delta\delta}) \qquad i = 1,2,3 \tag{3.5}$$

From system (3.5), six independent equations can be extracted (three from the last column of the matrices and three from the rotational part of the matrices). The equations have six dependent variables (θ^i_1, θ^i_2, θ^i_3, d^i_4, θ^i_5, θ^i_6), for given x, y, and z (coordinate of the point O_p in S_b). Then, by writing system (3.5) for all three legs, a system of 18 independent equations in 18 variables is obtained. The system obtained may admit many of 18-tuples solutions. By given a proper initial estimation of the solution, the actual 18-tuple solution (the one which is of practical interest) is obtained by the Newton-Raphson method. Thus, providing the values of the variables θ^i_3 and d^i_4, i =1,2,3, for each of the i-th leg.

The third step is to use the axial, k_{ai}, i =1,2,3, and the rotational, k_{ri}, i = 1,2,3, stiffnesses of the i-th leg in order to compute the value of the axial force f_i, i = 1,2,3, along $\mathbf{s}_i$, and the moment m_i, i = 1,2,3, around $\mathbf{u}_i$, respectively related to the displacement d^i_4, i = 1,2,3, and the rotation θ^i_3, i = 1,2,3, of the i-th leg:

$$f_i = k_{ai}.d_4^i \qquad i=1,2,3 \tag{3.6}$$

$$m_i = \frac{k_{ri}.\theta_3^i}{\cos\varphi_i} \qquad i=1,2,3 \tag{3.7}$$

where φ_i, i = 1,2,3, is the angle between the unit vectors $\mathbf{s}_i$ and $\mathbf{u}_i$. By choosing an annular section of the leg, the axial and the rotational stiffnesses k_{ai} and k_{ri} can be computed as follows:

$$k_{ai} = \frac{\pi E_i\left(R^2_{ext,i} - R^2_{int,i}\right)}{l_i} \qquad i=1,2,3 \tag{3.8}$$

$$k_{ri} = \frac{G_i I_{0i}}{l_i} \qquad i=1,2,3 \tag{3.9}$$

where E_i and G_i are respectively the Young and the Coulomb modules of the i-th leg; $R_{ext,i}$ and $R_{int,i}$ are the external and the internal radii of the annular section of the i-th leg; I_{0i} is the polar moment of inertia of the i-th leg and l_i is the i-th leg actual length.

The fourth step is to compute the external forces **F**, and the external moments **M**, applied at the reference point O_p of the platform as shown in Fig. 3.3, which correspond to the first column of the stiffness matrix **H**, by using the following equation [22]:

$$\begin{bmatrix} \mathbf{S} & \mathbf{0} \\ \mathbf{R} & \mathbf{U} \end{bmatrix} \begin{bmatrix} f_1 & f_2 & f_3 & m_1 & m_2 & m_3 \end{bmatrix}^T = \begin{bmatrix} \mathbf{F} \\ \mathbf{M} \end{bmatrix} \tag{3.10}$$

where:

$$\mathbf{S} = \begin{bmatrix} \mathbf{s}_1 & \mathbf{s}_2 & \mathbf{s}_3 \end{bmatrix} \tag{3.11}$$

$$\mathbf{R} = \begin{bmatrix} \mathbf{r}_{p1} \times \mathbf{s}_1 & \mathbf{r}_{p2} \times \mathbf{s}_2 & \mathbf{r}_{p3} \times \mathbf{s}_3 \end{bmatrix} \tag{3.12}$$

$$\mathbf{U} = \begin{bmatrix} \mathbf{u}_1 & \mathbf{u}_2 & \mathbf{u}_3 \end{bmatrix} \tag{3.13}$$

$$\mathbf{r}_{pi} = \overrightarrow{O_p A_i} \qquad i = 1,2,3 \tag{3.14}$$

The fifth step is to repeat the three previous steps (from the second to the fourth) to compute, analogously to what done for the first column, the second, the third, the fourth, the fifth and the sixth column of the stiffness matrix **H**. This can be performed by imposing respectively a translation of one unit and a rotation of one unit as well in all and around all directions, that is by imposing $\mathbf{\Delta}\gamma=(0,1,0,0,0,0)^T$, $\mathbf{\Delta}\gamma=(0,0,1,0,0,0)^T$, …, $\mathbf{\Delta}\gamma=(0,0,0,0,0,1)^T$.

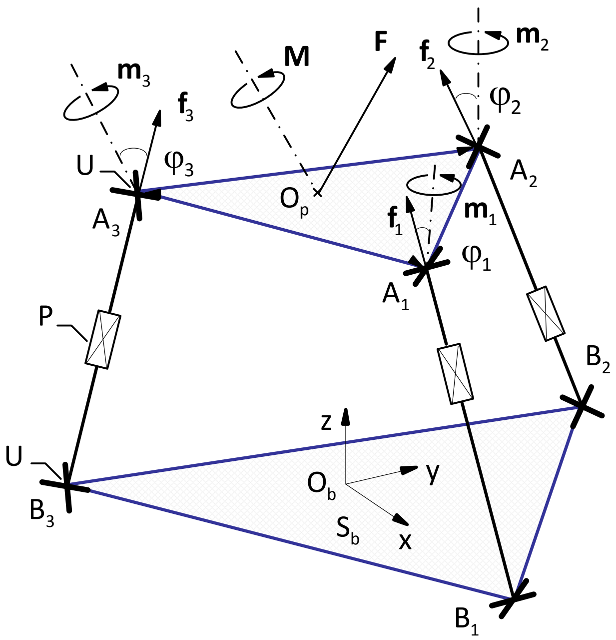

Figure 3.3. *Different forces and moments applied on the reference point Op of the platform of the 3-UPU TPM*

At this stage a stiffness index can be defined. The determinant of the stiffness matrix **H** cannot be taken as a stiffness index because it has components which do not have the same units [27]. One of the best alternatives is to make partition of the stiffness matrix **H** computed above in four 3x3 matrices $\mathbf{H}_k$ (components of $\mathbf{H}_k$, k = 1,2,3,4, have the same units) as follows [28]:

$$\mathbf{H} = \begin{bmatrix} \mathbf{H}_1 & \mathbf{H}_2 \\ \mathbf{H}_3 & \mathbf{H}_4 \end{bmatrix} \tag{3.15}$$

Then, the stiffness indexes sf_k, k = 1,2,3,4, correspond to the absolute value of the determinants of the four 3x3 matrices $\mathbf{H}_k$, k = 1,2,3,4, and consider them independently.

The two indexes sf_1 and sf_2 represent respectively the stiffness of the manipulator to the translation and the rotation of its platform due to the external force **F**. While the indexes sf_3 and sf_4 represent respectively the stiffness of the manipulator to the translation and the rotation of its platform due to the external moment **M**.

3.1.2. Procedure to compute an upper bound for the variation of the rate (bending moment/torque) applied on each leg of the 3-UPU TPM in the whole workspace

In this section, a procedure that computes an upper bound for the variation of the absolute value of the rate between the bending moment and the torque applied on each leg of the 3-UPU TPM in the whole workspace is presented.

The moment m_i, i = 1,2,3, applied by the platform to the i-th leg about the vector $\mathbf{u}_i$, orthogonal to the cross link of the universal joint (can be computed by the static analysis of the manipulator) can be decomposed in two moments, the torque m_{ti}, i = 1,2,3, about the direction of the leg $\mathbf{s}_i$ and the bending moment m_{bi}, i = 1,2,3, about a direction $\mathbf{b}_i$ orthogonal to the plane defined by the vectors $\mathbf{s}_i$ and $\mathbf{u}_i$ as shown in Fig. 3.4:

$$m_i\mathbf{u}_i = m_{ti}\mathbf{s}_i + m_{bi}\mathbf{b}_i \qquad i = 1,2,3 \tag{3.16}$$

where the torque m_{ti}, i = 1,2,3, and the bending moment m_{bi}, i = 1,2,3, can be expressed as:

$$m_{ti} = m_i \cos\varphi_i \qquad i = 1,2,3 \tag{3.17}$$

$$m_{bi} = m_i \sin\varphi_i \qquad i = 1,2,3 \tag{3.18}$$

where φ_i is the angle between the unit vectors $\mathbf{s}_i$ and $\mathbf{u}_i$.

The absolute value of the rate μ_i, i = 1,2,3, between the bending moment m_{bi}, and the torque m_{ti}, applied on the i-th leg is given as follows:

$$|\mu_i| = \left|\frac{\sin\varphi_i}{\cos\varphi_i}\right| \qquad i = 1,2,3 \tag{3.19}$$

The core of the procedure is to compute an upper bound for the variation of the rate μ_i, i = 1,2,3, for each of the i-th leg of the manipulator, in the whole workspace. This procedure is composed of four main steps.

The first step is to envelope the given workspace by a sphere S which locate it above the plane π (defined as in Chapter 1) and placed inside a closed surface K = K_d, where K_d is a given value of the determinant of the Jacobian matrix **J**.

Then, the second step is to express the rate μ_i, i = 1,2,3, function of the angle ω_i which corresponds to the angle formed by the unit vectors $\mathbf{s}_i$ and the unit vector of the direction of the revolute joint connected the i-th leg to the base, $\mathbf{q}_{1i}$, as shown in Fig. 3.4. First, according to a routine done and given in Appendix B, the relationship between the two angles φ_i and ω_i corresponds to:

$$\cos\varphi_i = \pm\sin\omega_i \qquad i = 1,2,3 \tag{3.20}$$

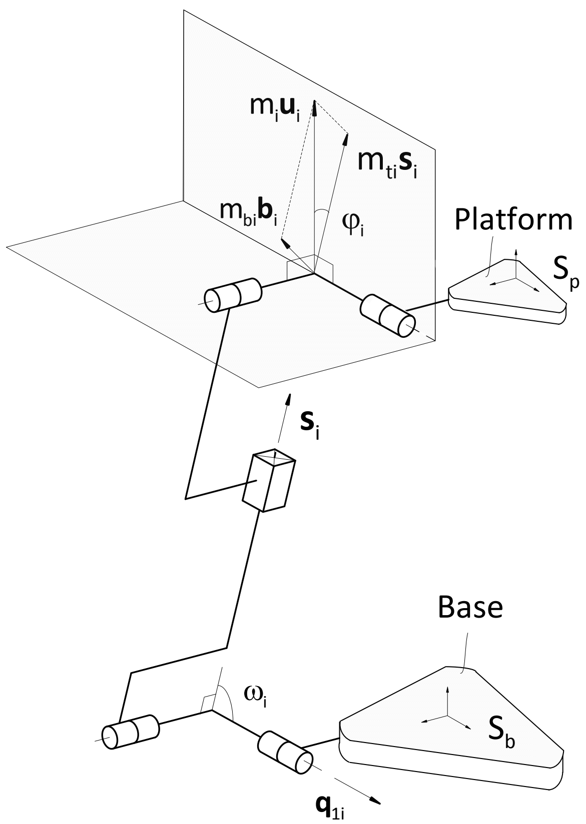

Figure 3.4. *The i-th leg of the 3-UPU TPM*

According to Eqs. (3.19, 3.20), the absolute value of the rate μ_i, i = 1,2,3, can be written as:

$$|\mu_i| = \left|\frac{\cos\omega_i}{\sin\omega_i}\right| \qquad i = 1,2,3 \tag{3.21}$$

The third step is to determine the expression of the absolute value of the rate μ_i, i = 1,2,3, function of the coordinate of the reference point O_p of the platform and the radii b and p (the radii of the two circles, which the center of the universal joints in the base and the platform respectively belong to). The expression of cosine of ω_i, i = 1,2,3, corresponds to the scalar product of the two unit vectors $\mathbf{q}_{1i}$ and $\mathbf{s}_i$. The expression of the unit vector $\mathbf{s}_i$ for the architecture of type A and type B are given as follows:

$$\begin{cases} \mathbf{s}_i = \dfrac{\begin{bmatrix} N_i & P_i & z \end{bmatrix}^T}{\left(N_i^2 + P_i^2 + z^2\right)^{1/2}} & i = 1,2,3, \quad \text{architectures of type A} \\ \mathbf{s}_i = \dfrac{\begin{bmatrix} R_i & T_i & z \end{bmatrix}^T}{\left(R_i^2 + T_i^2 + z^2\right)^{1/2}} & i = 1,2,3, \quad \text{architectures of type B} \end{cases} \tag{3.22}$$

where:

$$N_i = x - (b - p)\cos\xi_i \qquad i = 1,2,3 \tag{3.23}$$

$$P_i = y - (b - p)\sin\xi_i \qquad i = 1,2,3 \tag{3.24}$$

$$R_i = x - (b + p)\cos\xi_i \qquad i = 1,2,3 \tag{3.25}$$

$$T_i = y - (b + p)\sin\xi_i \qquad i = 1,2,3 \tag{3.26}$$

x, y and z are the coordinates of reference point O_p of the platform in the system S_b fixed to the base and ξ_i, i = 1,2,3, is the angle between the x-axis of S_b and the vector O_bB_i.

The unit vectors $\mathbf{q}_{1i}$, (i = 1,2,3, for the architectures 1.A, 1.B, 2.A, 2.B and i = 1,2, for the architectures 3.A, 3.B, 4.A, 4.B) of the direction of the revolute joint connected the i-th leg to the base are coplanar and belongs the plane π (z = 0) can be written as:

$$\mathbf{q}_{1i} = \begin{bmatrix} \kappa_{1i} & \lambda_{1i} & 0 \end{bmatrix}^T \qquad \begin{cases} i = 1,2,3, \ \text{architectures 1.A,1.B,2.A,2.B} \\ i = 1,2, \ \text{architectures 3.A,3.B,4.A,4.B} \end{cases} \tag{3.27}$$

where:

$$\lambda_{1i} = \pm\left(1-\kappa_{1i}^2\right)^{1/2} \tag{3.28}$$

κ_{1i} is the x component of the unit vector $\mathbf{q}_{1i}$ in the system S_b. The value of κ_{1i} depends to the architecture chosen and ranges from -1 to 1.
For the architectures 3.A, 3.B, 4.A and 4.B, the unit vectors $\mathbf{q}_{13}$, of the direction of the revolute joint connected the leg 3 to the base is orthogonal to the plane π (z = 0):

$$\mathbf{q}_{13} = \begin{bmatrix} 0 & 0 & 1 \end{bmatrix}^T \tag{3.29}$$

According to the Eqs. (3.22, 3.27, 3.29), the expression of cosines of the angles ω_i, i = 1,2,3, for the different architectures is obtained as follows:

$$\begin{cases} \cos\omega_i = \dfrac{\kappa_{1i}N_i + \lambda_{1i}P_i}{\left(N_i^2 + P_i^2 + z^2\right)^{1/2}} & \begin{cases} i=1,2,3, \text{ architectures } 1.A, 2.A \\ i=1,2, \text{ architectures } 3.A, 4.A \end{cases} \\ \cos\omega_i = \dfrac{\kappa_{1i}R_i + \lambda_{1i}T_i}{\left(R_i^2 + T_i^2 + z^2\right)^{1/2}} & \begin{cases} i=1,2,3, \text{ architectures } 1.B, 2.B \\ i=1,2, \text{ architectures } 3.B, 4.B \end{cases} \\ \cos\omega_3 = \dfrac{z}{\left(N_3^2 + P_3^2 + z^2\right)^{1/2}} & \text{architectures } 3.A, 4.A \\ \cos\omega_3 = \dfrac{z}{\left(R_3^2 + T_3^2 + z^2\right)^{1/2}} & \text{architectures } 3.B, 4.B \end{cases} \tag{3.30}$$

Thus, by substituting the cosine of the angle ω_i, i = 1,2,3, given by Eqn. (3.30) in Eqn. (3.21), the rate μ_i, i = 1,2,3, for the different architectures are computed and given by the following equation:

$$\begin{cases} \mu_i = \left(\dfrac{\kappa_{1i}^2 N_i^2 + \lambda_{1i}^2 P_i^2 + 2\kappa_{1i}\lambda_{1i}N_iP_i}{\lambda_{1i}^2 N_i^2 + \kappa_{1i}^2 P_i^2 - 2\kappa_{1i}\lambda_{1i}N_iP_i + z^2}\right)^{1/2} & \begin{cases} i=1,2,3, \text{ for the architectures } 1.A, 2.A \\ i=1,2, \text{ for the architectures } 3.A, 4.A \end{cases} \\ \mu_i = \left(\dfrac{\kappa_{1i}^2 R_i^2 + \lambda_{1i}^2 T_i^2 + 2\kappa_{1i}\lambda_{1i}R_iT_i}{\lambda_{1i}^2 R_i^2 + \kappa_{1i}^2 T_i^2 - 2\kappa_{1i}\lambda_{1i}R_iT_i + z^2}\right)^{1/2} & \begin{cases} i=1,2,3, \text{ for the architectures } 1.B, 2.B \\ i=1,2, \text{ for the architectures } 3.B, 4.B \end{cases} \\ \mu_3 = \dfrac{z}{\left(N_3^2 + P_3^2\right)^{1/2}} & \text{for the architectures } 3.A, 4.A \\ \mu_3 = \dfrac{z}{\left(R_3^2 + T_3^2\right)^{1/2}} & \text{for the architectures } 3.B, 4.B \end{cases} \tag{3.31}$$

The fourth step is the following:

- According to the first two equations of Eqn. (3.31), the rate μ_i, (i = 1,2,3, for the architectures 1.A, 1.B, 2.A , 2.B and i = 1,2, for the architectures 3.A, 3.B, 3.A , 3.B) is inversely proportional to the value of z coordinate of the reference point O_p of the platform, but also it depends to the value of x and y coordinates of the point O_p. Thus, the upper bound for the variation of this rate in the whole workspace, corresponds to the maximum value of μ_i in the biggest section W of the sphere S (its normal is the z axis of S_b) and insert it for the lowest value of z as shown in Fig. 3.5-a.
- According to the last two equations of Eqn. (3.31), the rate μ_3, for the architectures 3.A, 3.B, 4.A and 4.B is proportional to the value of z coordinate of the reference point O_p of the platform, but also it depends to the value of x and y coordinates of the point O_p. Thus, the upper bound for the variation of this rate in the whole workspace corresponds to the maximum value of μ_3 in the biggest section W of the sphere S (its normal is the z axis of S_b) and insert it for the biggest value of z as shown in Fig. 3.5-b.

3.2. Maximum platform position error caused by the clearance in the revolute joints of the 3-UPU TPM

In this section, the analytic expression of the manipulator pose error caused by the axial and radial clearance in the revolute joints, for a given external wrench applied on the reference point O_p of the platform is recalled. In addition, a numerical procedure to find the maximum of the platform position error is presented by the optimization of an

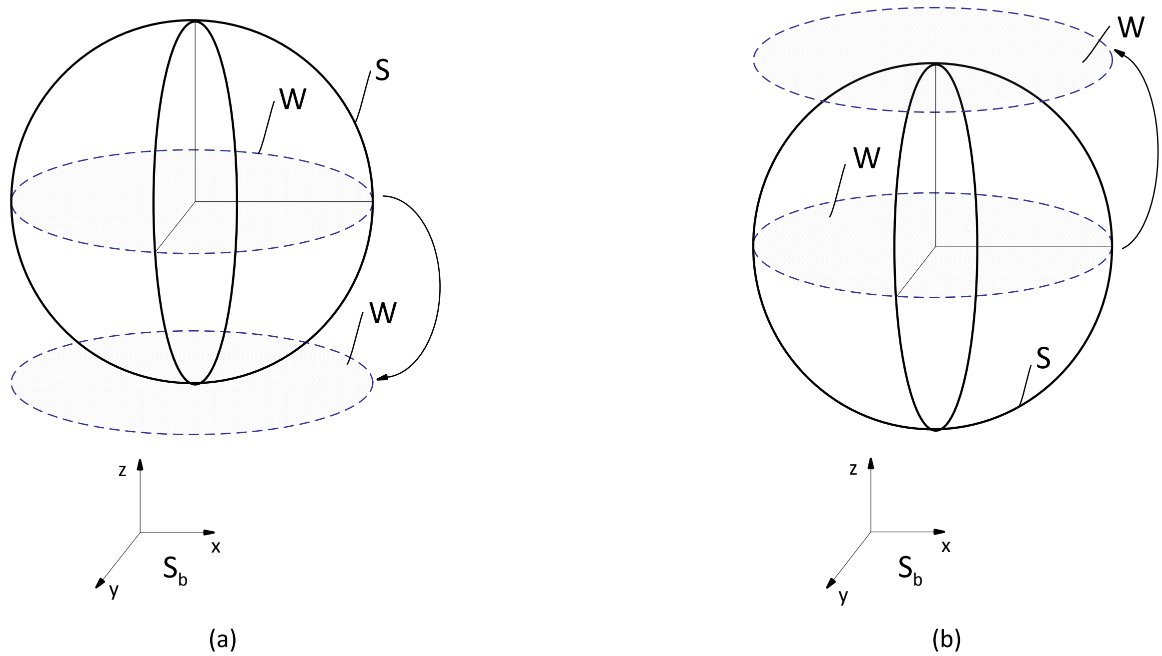

Figure 3.5. *Location of the section W of the workspace for computing the upper bound of the rate bending moment/torque applied on each leg*

objective function defined as the negative of the absolute value of the platform position error. The obtained maximum platform position error, is considered as the clearance index and can be used in order to apply the procedure defined in Chapter 2.

3.2.1. Expression of the pose error of the platform caused by the clearance in the revolute joints

The virtual work method is used in order to find the relation between the platform pose error and the axial and radial clearance considered in the revolute joints (the clearance is not considered on the actuated prismatic joints). The superposition method is used in order to quantify the pose error induced by all the joints clearances. Moreover, the joint displacement will be presented as a function of the contact forces [29-36].
According to Eqn. (3.10), the wrenches supported by the three legs are given by:

$$\begin{bmatrix} f_1 & f_2 & f_3 & m_1 & m_2 & m_3 \end{bmatrix}^T = \begin{bmatrix} \mathbf{S}^{-1} & \mathbf{0} \\ -\mathbf{U}^{-1}\mathbf{R}\mathbf{S}^{-1} & \mathbf{U}^{-1} \end{bmatrix} \begin{bmatrix} \mathbf{F} \\ \mathbf{M} \end{bmatrix} \tag{3.32}$$

where the 3x3 matrices **S**, **R** and **U** (the matrices **U** and **S** are fully ranked) are defined respectively by Eqs. (3.11, 3.12, 3.13).
Then, the wrench, $\boldsymbol{\tau}_i$, i = 1,2,3, applied by the platform to the i-th leg, which formed by an axial force f_i and a moment m_i around the unit vector $\mathbf{u}_i$, is expressed by the following equation:

$$\boldsymbol{\tau}_i = \mathbf{G}_i \boldsymbol{\tau}_{ext} \qquad i=1,2,3 \tag{3.33}$$

where:

$$\boldsymbol{\tau}_{ext} = \begin{bmatrix} \mathbf{F} \\ \mathbf{M} \end{bmatrix} \tag{3.34}$$

$$\mathbf{G}_i = \begin{bmatrix} \mathbf{s}_i & 0 \\ 0 & \mathbf{u}_i \end{bmatrix} \begin{bmatrix} l_i \\ l_{i+3} \end{bmatrix} \qquad i=1,2,3 \tag{3.35}$$

l_i and l_{i+3} are respectively the i-th and (i+3)th line vectors (1x6) from the (6x6) matrix defined by Eqn. (3.32).
Figure 3.6 shows the axial, ε_a, and radial, ε_d, clearance in the j-th revolute joint connected to the i-th leg of the manipulator.

Two local reference systems are considered respectively fixed to the two links of the revolute pair (at the actual manipulator configuration) with their origins in the middle of the pair pin (with axial length 2L) at point A_i, i = 1,2,3, of the revolute pair axis (Fig. 3.6), and with x, y axes and z axis respectively orthogonal to and along the revolute axis.

The wrench $\boldsymbol{\tau}_i$, i = 1,2,3, transmitted by the revolute joint can be transformed into an equivalent system to three contact forces [29,30,31]. Namely, $\boldsymbol{\sigma}_{1,ji}$ and $\boldsymbol{\sigma}_{2,ji}$, (i = 1,2,3; j = 1,2,3,4) perpendicular to the axis of the revolute joint and belonging to the trust plane of the joint (a plane through the revolute axis), and $\sigma_{3,ji}.\mathbf{q}_{ji}$ along the revolute joint axis.
The three forces in the local systems are given by [29,30,31]:

$$\begin{cases} \boldsymbol{\sigma}_{1,ji} = \mathbf{W}_{1,ji}\boldsymbol{\tau}_i \\ \boldsymbol{\sigma}_{2,ji} = \mathbf{W}_{2,ji}\boldsymbol{\tau}_i \\ \sigma_{3,ji}\mathbf{q}_{ji} = \mathbf{W}_{3,ji}\boldsymbol{\tau}_i \end{cases} \qquad i = 1,2,3;\ \ j = 1,2,3,4 \tag{3.36}$$

where $\mathbf{W}_{1,ji}$ and $\mathbf{W}_{2,ji}$ are 3x6 matrices and $\mathbf{W}_{3,ji}$ is a vector of six components, which depend to the architecture and the configuration of the manipulator (the analytic expression of the matrices $\mathbf{W}_{1,ji}$, $\mathbf{W}_{2,ji}$ and $\mathbf{W}_{3,ji}$, i = 1,2,3; j = 1,2,3,4, are given in Appendix B).
The Principal of Virtual Work gives:

$$\boldsymbol{\tau}_{ext}^T \boldsymbol{\Delta\Gamma}_{ji} + \sum_{k=1}^{3} \boldsymbol{\sigma}_{k,ji}^T \boldsymbol{\Delta}\mathbf{r}_{k,ji} = 0 \qquad i = 1,2,3;\ \ j = 1,2,3,4 \tag{3.37}$$

where $\boldsymbol{\Delta}\mathbf{r}_{k,ji}$, (i = 1,2,3; j = 1,2,3,4; k = 1,2,3) are the infinitesimal displacements of the application points of the forces $\boldsymbol{\sigma}_{1,ji}$, $\boldsymbol{\sigma}_{2,ji}$ and $\sigma_{3,ji}.\mathbf{q}_{ji}$ and $\boldsymbol{\Delta\Gamma}_{ji}$, is the corresponding platform pose error caused by the clearance in the j-th revolute joint of the i-th leg.

The displacements $\boldsymbol{\Delta}\mathbf{r}_{k,ji}$, (i = 1,2,3; j = 1,2,3,4; k = 1,2,3) can be assumed as vectors with the same direction as $\boldsymbol{\sigma}_{k,ji}$ and opposite versus. Their magnitude is the clearance value (ε_d for $\boldsymbol{\sigma}_{1,ji}$ and $\boldsymbol{\sigma}_{2,ji}$, ε_a for $\sigma_{3,ji}.\mathbf{q}_{ji}$):

$$\begin{cases} \boldsymbol{\Delta}\mathbf{r}_{1,ji} = -\varepsilon_d \dfrac{\boldsymbol{\sigma}_{1,ji}}{\left\| \boldsymbol{\sigma}_{1,ji} \right\|} \\ \boldsymbol{\Delta}\mathbf{r}_{2,ji} = -\varepsilon_d \dfrac{\boldsymbol{\sigma}_{2,ji}}{\left\| \boldsymbol{\sigma}_{2,ji} \right\|} \\ \boldsymbol{\Delta}\mathbf{r}_{3,ji} = -\varepsilon_a \dfrac{\sigma_{3,ji}\mathbf{q}_{ji}}{\left\| \sigma_{3,ji}\mathbf{q}_{ji} \right\|} \end{cases} \qquad i = 1,2,3;\ \ j = 1,2,3,4 \tag{3.38}$$

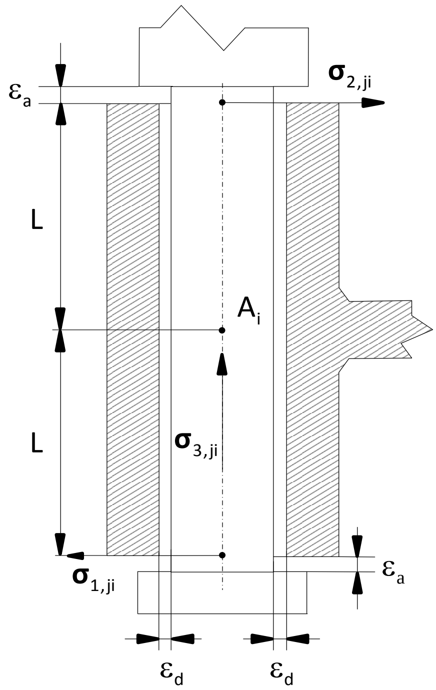

Figure 3.6. *Clearances in the j-th revolute joint connected to the i-th leg*

By substituting the expression of $\mathbf{\Delta r}_{k,ji}$, (i = 1,2,3; j = 1,2,3,4; k = 1,2,3) given by Eqn. (3.38), the expression of the forces $\boldsymbol{\sigma}_{1,ji}$, $\boldsymbol{\sigma}_{2,ji}$ and $\sigma_{3,ji}.\mathbf{q}_{ji}$ given by Eqn. (3.36), and the expression of $\boldsymbol{\tau}_i$, i = 1,2,3, given by Eqn. (3.33), in Eqn. (3.37):

$$\boldsymbol{\tau}_{ext}^{T}\left(\mathbf{\Delta\Gamma}_{ji}-\mathbf{G}_i^{T}\left(\varepsilon_d\mathbf{W}_{1,ji}^{T}\frac{\mathbf{W}_{1,ji}\mathbf{G}_i\boldsymbol{\tau}_{ext}}{\left\|\mathbf{W}_{1,ji}\mathbf{G}_i\boldsymbol{\tau}_{ext}\right\|}+\varepsilon_d\mathbf{W}_{2,ji}^{T}\frac{\mathbf{W}_{2,ji}\mathbf{G}_i\boldsymbol{\tau}_{ext}}{\left\|\mathbf{W}_{2,ji}\mathbf{G}_i\boldsymbol{\tau}_{ext}\right\|}+\varepsilon_a\mathbf{W}_{3,ji}^{T}\frac{\mathbf{W}_{3,ji}\mathbf{G}_i\boldsymbol{\tau}_{ext}}{\left\|\mathbf{W}_{3,ji}\mathbf{G}_i\boldsymbol{\tau}_{ext}\right\|}\right)\right)=0 \tag{3.39}$$

Equation (3.39) holds regardless of the external load acting on the mechanism, and can be arranged as:

$$\mathbf{\Delta\Gamma}_{ji}=\mathbf{G}_i^{T}\left(\varepsilon_d\mathbf{W}_{1,ji}^{T}\frac{\mathbf{W}_{1,ji}\mathbf{G}_i\boldsymbol{\tau}_{ext}}{\left\|\mathbf{W}_{1,ji}\mathbf{G}_i\boldsymbol{\tau}_{ext}\right\|}+\varepsilon_d\mathbf{W}_{2,ji}^{T}\frac{\mathbf{W}_{2,ji}\mathbf{G}_i\boldsymbol{\tau}_{ext}}{\left\|\mathbf{W}_{2,ji}\mathbf{G}_i\boldsymbol{\tau}_{ext}\right\|}+\varepsilon_a\mathbf{W}_{3,ji}^{T}\frac{\mathbf{W}_{3,ji}\mathbf{G}_i\boldsymbol{\tau}_{ext}}{\left\|\mathbf{W}_{3,ji}\mathbf{G}_i\boldsymbol{\tau}_{ext}\right\|}\right) \tag{3.40}$$

Thus, the overall displacement $\mathbf{\Delta\Gamma}$, of the platform due to the clearance in the revolute joints can be determined by adding all the effects (provided clearance is very small and a linear approximation is acceptable):

$$\mathbf{\Delta\Gamma}=\sum_{i=1}^{3}\mathbf{G}_i^{T}\sum_{j=1}^{4}\left(\varepsilon_d\mathbf{W}_{1,ji}^{T}\frac{\mathbf{W}_{1,ji}\mathbf{G}_i\boldsymbol{\tau}_{ext}}{\left\|\mathbf{W}_{1,ji}\mathbf{G}_i\boldsymbol{\tau}_{ext}\right\|}+\varepsilon_d\mathbf{W}_{2,ji}^{T}\frac{\mathbf{W}_{2,ji}\mathbf{G}_i\boldsymbol{\tau}_{ext}}{\left\|\mathbf{W}_{2,ji}\mathbf{G}_i\boldsymbol{\tau}_{ext}\right\|}+\varepsilon_a\mathbf{W}_{3,ji}^{T}\frac{\mathbf{W}_{3,ji}\mathbf{G}_i\boldsymbol{\tau}_{ext}}{\left\|\mathbf{W}_{3,ji}\mathbf{G}_i\boldsymbol{\tau}_{ext}\right\|}\right) \tag{3.41}$$

By the condition of the pure translation of the platform, which corresponds to the axes of the two intermediate revolute pairs in the i-th leg are parallel to each other ($\mathbf{q}_{2i}$ = $\mathbf{q}_{3i}$, i = 1,2,3) and the axes of the two ending revolute pairs in the i-th leg are parallel to each other ($\mathbf{q}_{1i}$ = $\mathbf{q}_{4i}$, i = 1,2,3), it can be obtained that:

$$\begin{cases} \mathbf{W}_{k,2i} = \mathbf{W}_{k,3i} \\ \mathbf{W}_{k,1i} = \mathbf{W}_{k,4i} \end{cases} \quad i = 1,2,3;\ k = 1,2,3 \tag{3.42}$$

By taking into account the result obtained by Eqn. (3.42), the platform pose error due to the axial and radial clearance in the revolute joints given by Eqn. (3.41) can be rewritten as:

$$\mathbf{\Delta\Gamma} = 2\sum_{i=1}^{3}\mathbf{G}_i^T\sum_{j=1}^{2}\left(\varepsilon_d\mathbf{W}_{1,ji}^T\frac{\mathbf{W}_{1,ji}\mathbf{G}_i\boldsymbol{\tau}_{ext}}{\left\|\mathbf{W}_{1,ji}\mathbf{G}_i\boldsymbol{\tau}_{ext}\right\|} + \varepsilon_d\mathbf{W}_{2,ji}^T\frac{\mathbf{W}_{2,ji}\mathbf{G}_i\boldsymbol{\tau}_{ext}}{\left\|\mathbf{W}_{2,ji}\mathbf{G}_i\boldsymbol{\tau}_{ext}\right\|} + \varepsilon_a\mathbf{W}_{3,ji}^T\frac{\mathbf{W}_{3,ji}\mathbf{G}_i\boldsymbol{\tau}_{ext}}{\left\|\mathbf{W}_{3,ji}\mathbf{G}_i\boldsymbol{\tau}_{ext}\right\|}\right) \tag{3.43}$$

3.2.2. Numerical procedure to compute the maximum position error of the platform due to the clearance in the revolute joints

In this section, a numerical procedure to find the maximum of the position error of the platform due the clearance in the revolute joints by using a function from the MATLAB Optimisation Toolbox is presented.

The position error of the platform, E_p, caused by the clearance in the revolute joints, which depends to the external wrench applied on the platform $\boldsymbol{\tau}_{ext}$, is computed by the following equation:

$$E_p = \left(E_{px}^2 + E_{py}^2 + E_{pz}^2\right)^{1/2} \tag{3.44}$$

where E_{px}, E_{py} and E_{pz} are respectively the first, the second and the third component of the (6x1) vector $\mathbf{\Delta\Gamma}$ obtained by Eqn. (3.43).

The procedure to compute the maximum position error of the platform due to the clearance in the revolute joints is composed of three main steps.

The first one is the definition of an objective function as the negative of the absolute value of the platform position error:

func = - E_p (3.45)

The maximum of the platform position error E_p, numerically corresponds to the optimization of the objective function '*func*'. Thus, the second step is to define the optimization problem as follows:

$$\begin{cases} \min \ func(\mathbf{x}) \\ \mathbf{l}_b \ \leq \ \mathbf{x} \ \leq \ \mathbf{u}_b \end{cases} \tag{3.46}$$

where the objective function '*func*' is defined by Eqn. (3.45); $\mathbf{x}$ is the vector (6x1) of variables which represents the external wrench applied on the reference point O_p of the platform $\boldsymbol{\tau}_{ext}$; $\mathbf{l}_b$ and $\mathbf{u}_b$ are (6x1) vectors which correspond respectively the lower and the upper bounds of the value of the components of the external wrench $\boldsymbol{\tau}_{ext}$.
The function used from MATLAB Optimization Toolbox to solve the problem defined by Eqn. (3.46) is '*fmincon*' [37]. The goal of this function is to find a minimum of a constrained nonlinear multivariable function. Thus, '*fmincon*' solves the following problem:

$$\min \mathrm{f(x)} \text{ such that } \begin{cases} \mathrm{c}(\mathbf{x}) \leq 0 \\ \mathrm{c}_{eq}(\mathbf{x}) = 0 \\ \mathbf{A}.\mathbf{x} \leq \mathbf{b} \\ \mathbf{A}_{eq}.\mathbf{x} = \mathbf{b}_{eq} \\ \mathbf{l}_b \ \leq \ \mathbf{x} \ \leq \ \mathbf{u}_b \end{cases} \tag{3.47}$$

where $\mathbf{x}$, $\mathbf{b}$, $\mathbf{b}_{eq}$, $\mathbf{l}_b$, and $\mathbf{u}_b$ are respectively vector of variables, vector for non linear equality constraints, vector for linear equality constraints, vectors of lower bounds and vectors of upper bounds of the variables; $\mathbf{A}_{eq}$ and $\mathbf{A}$ are respectively matrices for linear and non linear equality constraints; f is the objective function to be minimized; c($\mathbf{x}$) and ceq($\mathbf{x}$) are two functions which can be nonlinear.

The function '*fmincon*' is based on the SQP (Sequential Quadratic Programming) algorithm. In this method, a Quadratic Programming subproblem is solved at each iteration. An estimate of the Hessian of the Lagrangian is updated at each iteration and a line search is performed using a merit function. The Quadratic Programming subproblem is solved using an active set strategy. The limitation of '*fmincon*' is the following:
- the objective function that is to be minimized and the constraints must be continuous functions.
- the obtained result is a minimum local.
- the objective function and the constraints functions must return real values.

The third step is to define the vectors of lower bound $\mathbf{l}_b$, and upper bounds $\mathbf{u}_b$ of the external wrench $\boldsymbol{\tau}_{ext}$ applied on the reference point O_p of the platform. Since the position error of the platform E_p, depends on the direction of the external wrench $\boldsymbol{\tau}_{ext}$, and does not depends on its module, the vectors $\mathbf{l}_b$ and $\mathbf{u}_b$ are defined as follows:

$$\mathbf{u}_b = -\mathbf{l}_b = \begin{bmatrix} 1 & 1 & 1 & 1 & 1 & 1 \end{bmatrix}^T \tag{3.48}$$

By using the value of the vectors $\mathbf{u}_b$ and $\mathbf{l}_b$ given by Eqn. (3.48), and taking an arbitrary initial point (initial guess) $\mathbf{x}_0$ of the vector of variable $\mathbf{x}$, the problem defined by Eqn. (3.46) can be solved. But the result obtained represents a minimum local of the objective function *'func'* and its absolute value corresponds to a maximum local of the position error of the platform E_p. One of the best alternatives to solve the problem, is to consider a combination of external wrench applied to the platform $\boldsymbol{\tau}_{ext}$, as initial guess (initial population). The value of each components of $\boldsymbol{\tau}_{ext}$ can be -1, 0, and 1, thus, the number of combination of the vector $\boldsymbol{\tau}_{ext}$ is equal to 3^6 = 729). Thus, the minimum chosen corresponds to the minimum of all the minimum local of *'func'* as shown in Fig. 3.7. The absolute value of the minimum chosen corresponds to the maximum position error of the platform due to the clearance in revolute joints which will be taken as clearance index in order to apply the procedure detailed in Chapter 2.

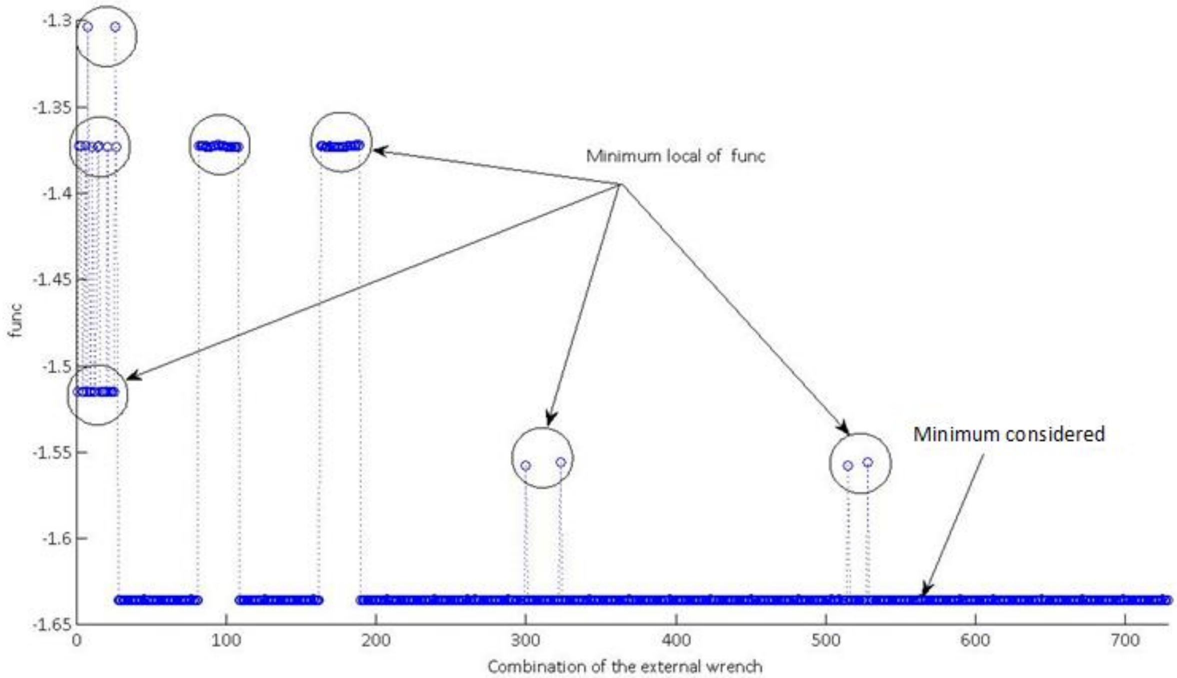

Figure 3.7. *Minimum local of the objective function 'func'*

Chapter 4: Results and discussion

This chapter reports the application of the procedure presented in the Chapter 2 for the selection of the best architecture of the 3-UPU TPMs among the eight ones (1.A, 1.B, 2.A, 2.B, 3.A, 3.B, 4.A and 4.B) as reported in Chapter 1 for a given task. The best architecture is selected based on each index in the first section and based on an objective function (a proper weighted selection of one or more indexes) in the second section of this chapter.

The given data are:

- the radius of the circle defined by the centers of the universal joint B_i, i = 1,2,3, connected to the platform: p = 45 mm.
- the security index K_d = 0.6.
- the diameter d_S of the sphere S that envelope the given workspace: d_S = 200 mm.
- the value of the angles ξ_i, i = 1,2,3, (angle between the x-axis of the reference system S_b and the vector O_bB_i): $\xi_1 = 0$; $\xi_2 = 2\pi/3$; $\xi_3 = 4\pi/3$.

For each leg:

- the offset used in order to avoid the collision of the legs for the architecture of type B: e = 30 mm.
- the external radius of the annular section of the leg: R_{ext} = 8 mm.
- the internal radius of the annular section of the leg: R_{int} = 5.5 mm.
- Young module (Aluminium): E = 69000 N/mm^2.
- Coulomb module (Aluminium): G = 26000 N/mm^2.

For each revolute joint:

- axial length: 2L = 60 mm
- axial clearance: ε_a = 0.1 mm
- radial clearance: ε_d = 0.1 mm

The directions of the base/platform revolute pairs axes of each architecture of the 3-UPU TPM, measured in S_b, are taken as:
* Architectures 1.A and 1.B: $\mathbf{q}_{1i}$, i = 1,2,3, are along the line tangent to the circle defined by the points B_i, i = 1,2,3:

$$\mathbf{q}_{11} = \begin{bmatrix} 0 \\ 1 \\ 0 \end{bmatrix}; \qquad \mathbf{q}_{12} = \begin{bmatrix} -\sin(2\pi/3) \\ \cos(2\pi/3) \\ 0 \end{bmatrix}; \qquad \mathbf{q}_{13} = \begin{bmatrix} -\sin(4\pi/3) \\ \cos(4\pi/3) \\ 0 \end{bmatrix} \tag{4.1}$$

* Architectures 2.A and 2.B:

$$\mathbf{q}_{11} = -\mathbf{q}_{13} = \begin{bmatrix} \cos(\pi/3) \\ -\sin(\pi/3) \\ 0 \end{bmatrix}; \qquad \mathbf{q}_{12} = \begin{bmatrix} \sin(\pi/3) \\ \cos(\pi/3) \\ 0 \end{bmatrix} \tag{4.2}$$

* Architectures 3.A and 3.B:

$$\mathbf{q}_{11} = \begin{bmatrix} \cos(\pi/3) \\ -\sin(\pi/3) \\ 0 \end{bmatrix}; \qquad \mathbf{q}_{12} = \begin{bmatrix} \sin(\pi/3) \\ \cos(\pi/3) \\ 0 \end{bmatrix}; \qquad \mathbf{q}_{13} = \begin{bmatrix} 0 \\ 0 \\ 1 \end{bmatrix} \tag{4.3}$$

* Architectures 4.A and 4.B:

$$\mathbf{q}_{11} = -\mathbf{q}_{13} = \begin{bmatrix} \cos(\pi/3) \\ -\sin(\pi/3) \\ 0 \end{bmatrix}; \qquad \mathbf{q}_{12} = \begin{bmatrix} 0 \\ 0 \\ 1 \end{bmatrix} \tag{4.4}$$

In order to avoid the collision of the legs for the architectures of type B (1.B, 2.B, 3.B and 4.B), the second of the three manufacturing solutions presented in section 1.3 of the Chapter 1 has been chosen. The value of the offset e, will be used only for these architectures in order to avoid the legs collision.

4.1. Selection of the best architecture of the 3-UPU TPM according to the indexes

This section presents the selection of the best architecture of the 3-UPU TPM presented in Chapter 1 according to each index proposed in Chapter 3. The size and the singularity loci of the manipulator are considered as two additional indexes.

4.1.1. Size of the 3-UPU TPM

By applying the first step of the procedure presented in Chapter 2, the coordinates of the center C_S of the sphere S expressed in the system S_b in [mm] for the architectures (1.A, 1.B), (2.A, 2.B), (3.A, 3.B) and (4.A, 4.B), are respectively (0, 0, 177.39), (50, -90, 218.125), (-27.5, 15, 348.6) and (0, 0, 172) in order to have the same security condition, $K \geq K_d$ (represents how far the manipulator is from a singularity configuration). Then, the computed rate b/p, is taken as manipulator size index, and given in Tab. 4.1 for each architecture of the manipulator. The best architecture corresponds to the minimum value of the rate b/p (small size of the manipulator). Thus, according to Tab. 4.1, the architecture 4.B is the best.

4.1.2. Singularity of the 3-UPU TPM

One of the frequently index used for the singularity of the manipulator, is the area A_ζ, inside the closed curve ζ obtained by intersection of the plane (parallel to the plane π defined in Chapter 1, and contain the center of the sphere C_S) with the closed surface $K = K_d$. Figures 4.1-a,b show a view of the shapes of the closed curves ζ and a (represents the curves of the section W chosen of the workspace) in the planes (x,z) and (x,y) respectively. The shape of the closed curve ζ changes according to the architecture of the manipulator. Indeed, architectures 1.A and 1.B (respectively (2.A and 2.B), (3.A and 3.B), (4.A and 4.B)) have the same shape of the closed curve ζ as shown in Fig. 4.1-c, since the closed surface $K = K_d$ depends on the directions of the unit vectors $\mathbf{s}_i$ and $\mathbf{u}_i$, i = 1,2,3, that are the same for these two architectures for the same platform position. To compute the area A_ζ, a square uniform mesh is considered for the section surrounded by the closed curves ζ. Then, the value of A_ζ is computed by an approximation:

$$A_\zeta = n_{pt} A_e \tag{4.5}$$

where A_e, the area of the mesh element (chosen too small in order to have a height precision of the value A_ζ) and n_{pt} is the number of the nodes inside the closed curve ζ.

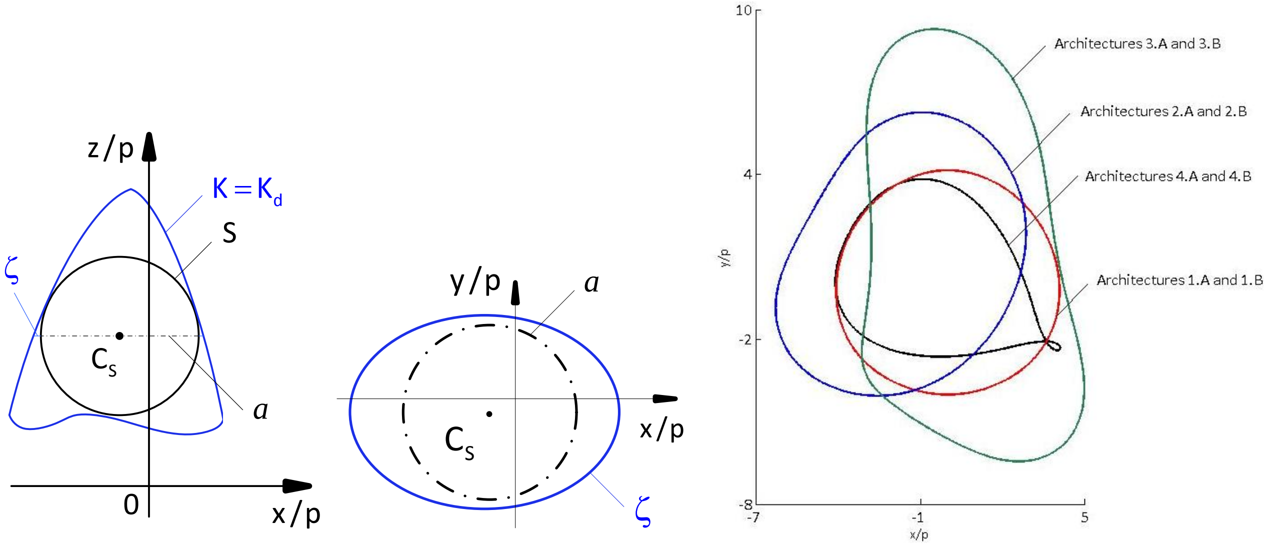

(a) (b) (c)

Figure 4.1. *(a) View of the shape of the closed curves a and ζ in the plane (x,z)*
(b) View of the shape of the closed curves a and ζ in the plane (x,y)
(c) View of the shape of the closed curve ζ for the different architectures in the plane (x,y)

Thus, the value of A_ζ, is computed for each architecture and given in Tab. 4.2. The best architecture corresponds to the maximum value of A_ζ, i.e., A_ζ measures the space where the reference point O_p of the platform moves on it and still keeping the same value of z (z is the coordinate of the point O_p in the system S_b, when the platform moves in the chosen section W of the workspace), and the same security condition $K \geq K_d$. Thus, according to the value of A_ζ, given in Tab. 4.2, the architectures 3.A and 3.B are the best.

4.1.3. Stiffness of the 3-UPU TPM

The distributions of the stiffness indexes sf_i, i = 1,2,3,4, (correspond to the absolute values of the determinants of the four 3x3 matrices $\mathbf{H}_i$, i = 1,2,3,4, defined in Chapter 3) of each architecture of the 3-UPU TPMs in the section W of the workspace are shown in Fig. 4.2-4.5. According to Eqn. (2.3), the values of the normalized stiffness indexes, T_{sfi}, i = 1,2,3,4, are computed for each architecture and reported in Tab. 4.3. The best architecture of the 3-UPU TPM corresponds to the maximum value of the normalized stiffness indexes, T_{sfi}, i = 1,2,3,4 (highest stiffness). From Tab. 4.3, it can be seen that the architecture of type B of the 3-UPU TPM have the highest stiffness to the rotation of the platform and the lowest stiffness to the translation of the platform itself due to the external force **F** applied on the platform than the corresponding architecture of type A. Thus, according to the values of normalized stiffness indexes T_{sf1} and T_{sf2}, the architecture 4.A and 4.B of the 3-UPU TPM have respectively the highest stiffness to the translation and the highest stiffness to the rotation of the platform due to the external force **F** applied on the platform itself. In addition, the architecture of type B of the 3-UPU TPM have the highest stiffness to the translation and the rotation of the platform due to the external moment **M** applied on the platform than the corresponding architecture of type A. Thus, according to the values of the normalized stiffness indexes T_{sf3} and T_{sf4}, the architecture 1.B have the highest stiffness to the translation and the rotation of the platform due to the external moment **M** applied on the platform itself.

4.1.4. Maximum position error of the platform due to the clearance in the revolute joints of the 3-UPU TPM

The distribution of the maximum platform position error due to the clearance in revolute joints (clearance index) E_p, of each architecture of the 3-UPU TPMs in the section W of the workspace (section W at z = 177.39 mm, z = 218.125 mm, z = 348.6 mm and z = 172 mm respectively for the architectures (1.A, 1.B), the architectures (2.A, 2.B), the architectures (3.A, 3.B), and the architectures (4.A, 4.B)) is shown in Fig. 4.6. Then, the value of the normalized clearance index, T_{Ep}, is computed for each architecture in Tab. 4.4. The best architecture corresponds to the minimum value of T_{Ep} (highest accuracy). Thus, the architecture 1.A is the best.

4.2. Selection of the best architecture of the 3-UPU TPM according to an objective function

In this section, an objective function defined by a proper weighted selection of the indexes defined above is presented. According to this objective function, a new selection of the best architecture of the 3-UPU TPM is done. The objective function *f*, is given by the following equation:

$$f = n_{sf_1} C_{sf_1} + n_{sf_2} C_{sf_2} + n_{sf_3} C_{sf_3} + n_{sf_4} C_{sf_4} + n_{A\zeta} C_{A\zeta} + n_{E_p} C_{E_p} + n_{b/p} C_{b/p} \tag{4.6}$$

where:

$$n_{sfi} = \frac{T_{sfi}}{\max\left(T_{sfi}\right)} \qquad i = 1,2,3,4 \tag{4.7}$$

$$n_{A\zeta} = \frac{A_\zeta}{\max\left(A_\zeta\right)} \tag{4.8}$$

$$n_{E_p} = \frac{\min\left(T_{E_p}\right)}{T_{E_p}} \tag{4.9}$$

$$n_{b/p} = \frac{\min(b/p)}{b/p} \tag{4.10}$$

and max(T_{sfi}), i = 1,2,3,4, and max(A_ζ), are respectively the maximum of the normalized values of the stiffness indexes, T_{sfi}, i = 1,2,3,4, and the maximum of the singularity index A_ζ, computed for the different architectures of the 3-UPU TPM; min(T_{Ep}) and min(b/p), are respectively the minimum of the normalized values of the clearance index T_{Ep}, and the maximum of the rate b/p (manipulator size index) computed for the different architectures of the 3-UPU TPM; C_{sfi}, i = 1,2,3,4, C_{Ep}, $C_{b/p}$ and $C_{A\zeta}$ are respectively the weight of the stiffness, clearance, the size of the manipulator and the singularity loci indexes, which depend to the task of the manipulator.
The best architecture of the 3-UPU TPM corresponds to the maximum value of the function *f*. According to a given task, the value of the weight of the different indexes is given as follows:

$$\begin{cases} C_{sfi} = 2 & i = 1,2,3,4 \\ C_{E_p} = 2 \\ C_{A\zeta} = 1 \\ C_{b/p} = 1 \end{cases} \tag{4.11}$$

By substituting the values of C_{sfi}, i = 1,2,3, C_{Ep}, $C_{A\zeta}$ and $C_{b/p}$ given by Eqn. (4.11) and the values of n_{sfi}, i = 1,2,3, n_{Ep}, $n_{A\zeta}$ and $n_{b/p}$ given in Tab. 4.5 into Eqn. (4.6), the objective function *f* is computed and given in Tab. 4.5. Thus, the architecture 1.B (*f* = 10.05) is the best for the 3-UPU TPM for doing the given task. In addition, it can be seen that the architectures of type B of the 3-UPU TPM are better than the corresponding architecture of type A.

Table 4.1. *The value of the rate b/p for each architecture*

Architectures / Size of the manipulator	1.A	1.B	2.A	2.B	3.A	3.B	4.A	4.B
b/p	5.81	3.81	7.25	5.25	10.1	8.1	5.15	3.15

Table 4.2. *The value of the area inside the closed curve ζ for each architecture*

Architectures / Singularity index	1.A	1.B	2.A	2.B	3.A	3.B	4.A	4.B
A_{ζ}, cm^2 [10^2]	10.52	10.52	14.05	14.05	19.59	19.59	7.26	7.26

Table 4.3. *The value of the normalized stiffness indexes T_{sfi}, i = 1,2,3,4, for each architecture*

Architectures / Stiffness indexes	1.A	1.B	2.A	2.B	3.A	3.B	4.A	4.B
T_{sf1}, N^2/mm^2 [10^{12}]	15	10.06	6.73	5.32	2.29	2.03	17.79	9.2
T_{sf2}, N^2/rad^2 [10^{14}]	6.74	$1.24\ 10^4$	2.52	$5.32\ 10^3$	0.97	$1.94\ 10^3$	9.22	$1.44\ 10^4$
T_{sf3}, N^2 [10^6]	1.97	$7.23\ 10^{11}$	0.92	$3.02\ 10^{11}$	0.22	$0.11\ 10^{10}$	3.13	$1.23\ 10^{11}$
T_{sf4}, N^2mm^2/rad^2 [10^{20}]	6.58	$8.54\ 10^2$	3.07	$3.09\ 10^2$	0.72	10.25	10.44	$1.95\ 10^2$

Table 4.4. *The value of the normalized clearance index T_{Ep} for each architecture*

Clearance index \ Architectures	1.A	1.B	2.A	2.B	3.A	3.B	4.A	4.B
T_{Ep} [mm]	1.41	1.56	1.53	1.82	1.58	1.71	1.62	1.98

Table 4.5. *The value of the objective function 'f' for each architecture*

Coefficient \ Architectures	1.A	1.B	2.A	2.B	3.A	3.B	4.A	4.B
$n_{b/p}$	0.54	0.83	0.44	0.6	0.31	0.39	0.61	1
$n_{A\zeta}$	0.54	0.54	0.72	0.72	1	1	0.37	0.37
n_{sf1}	0.84	0.57	0.38	0.3	0.13	0.11	1	0.52
n_{sf2}	$4.68\ 10^{-4}$	0.86	$1.75\ 10^{-4}$	0.47	$0.67\ 10^{-4}$	0.14	$6.4\ 10^{-4}$	1
n_{sf3}	$0.27\ 10^{11}$	1	$0.13\ 10^{11}$	0.42	$0.03\ 10^{11}$	0.02	$0.43\ 10^{11}$	0.17
n_{sf4}	$0.77\ 10^{-2}$	1	$0.36\ 10^{-2}$	0.36	$0.08\ 10^{-2}$	$1.2\ 10^{-2}$	$1.22\ 10^{-2}$	0.23
n_{Ep}	1	0.91	0.92	0.78	0.9	0.83	0.87	0.72
f	4.76	10.05	3.76	5.98	3.37	3.58	4.72	6.65

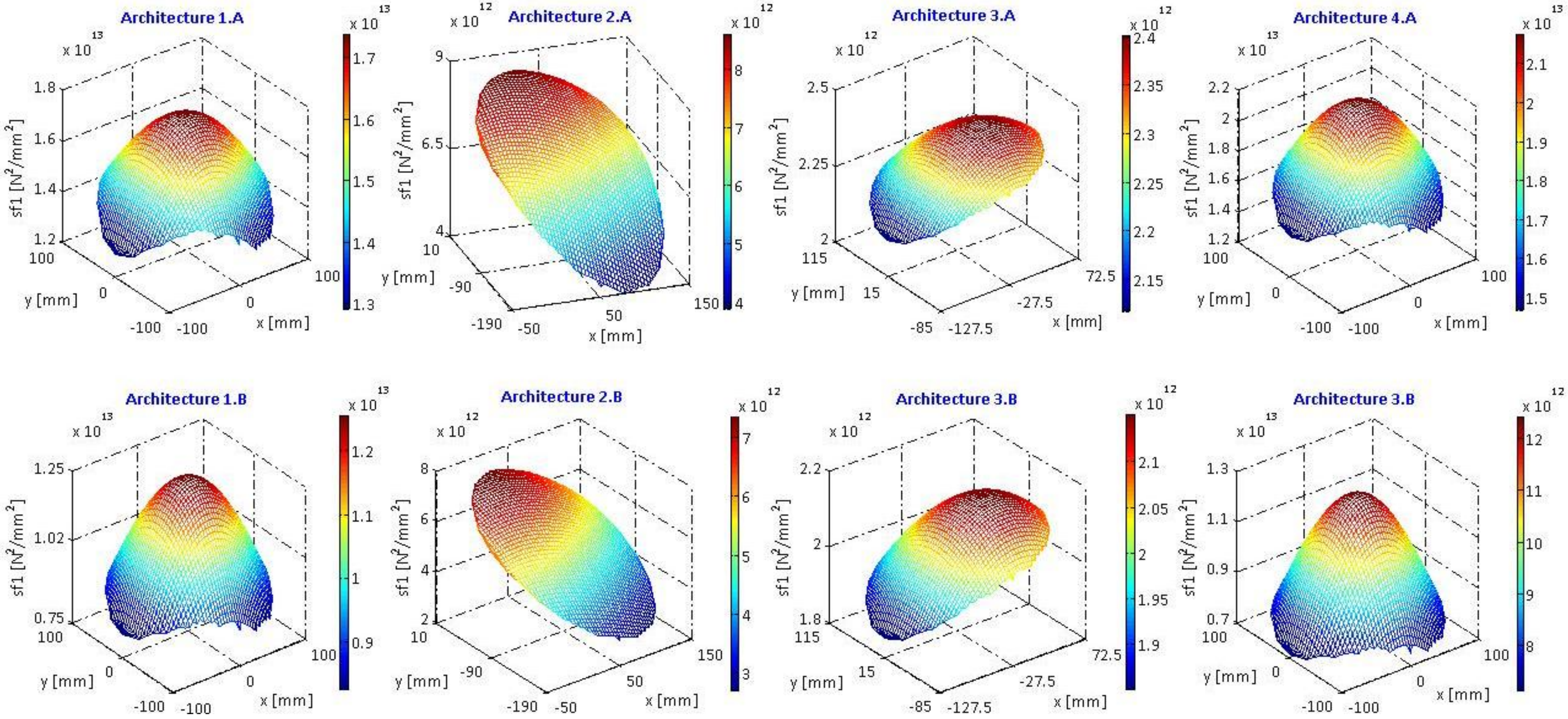

Figure 4.2. *Distribution of the stiffness index sf_1 in the section W of the workspace for each architecture of the 3-UPU TPM*

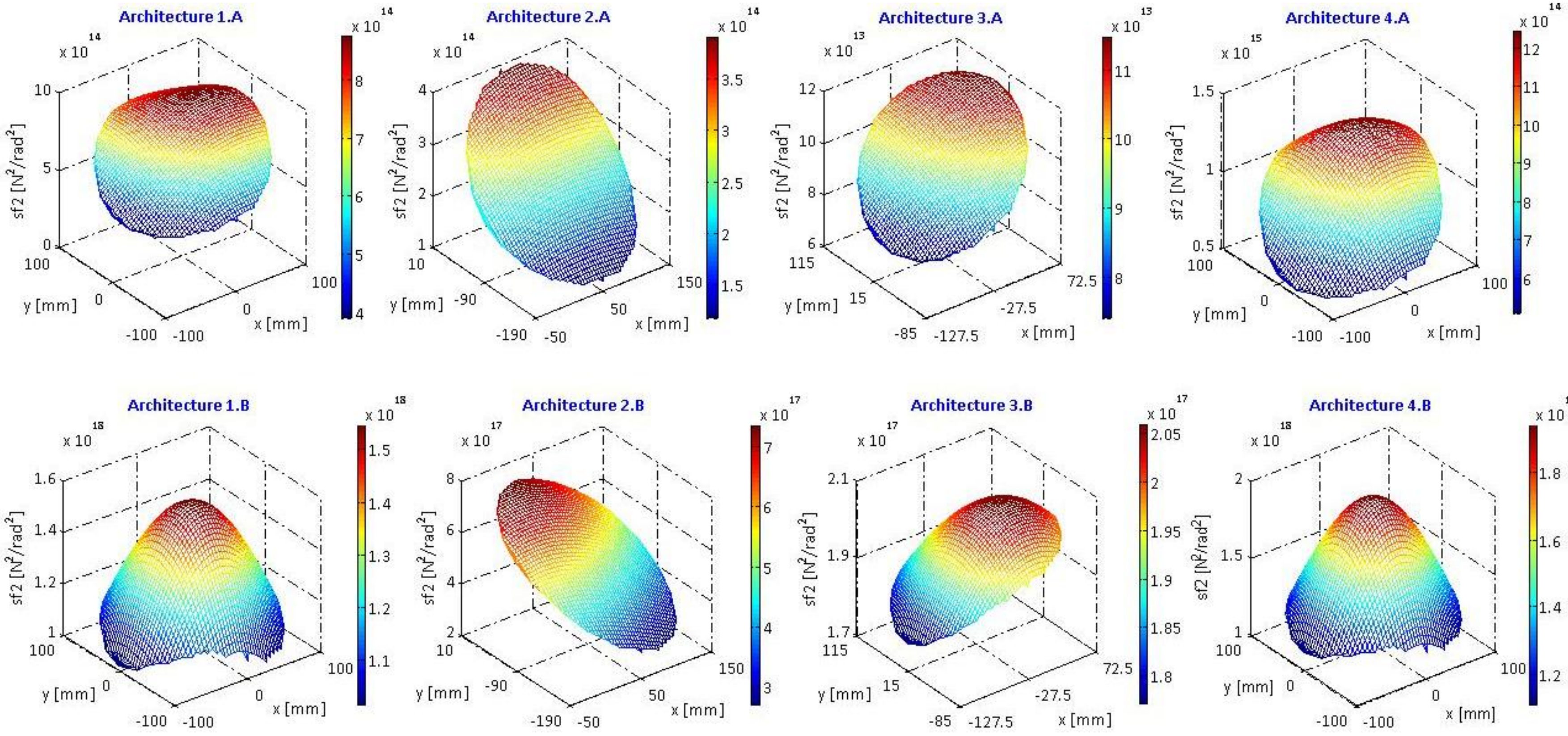

Figure 4.3. *Distribution of the stiffness index sf_2 in the section W of the workspace for each architecture of the 3-UPU TPM*

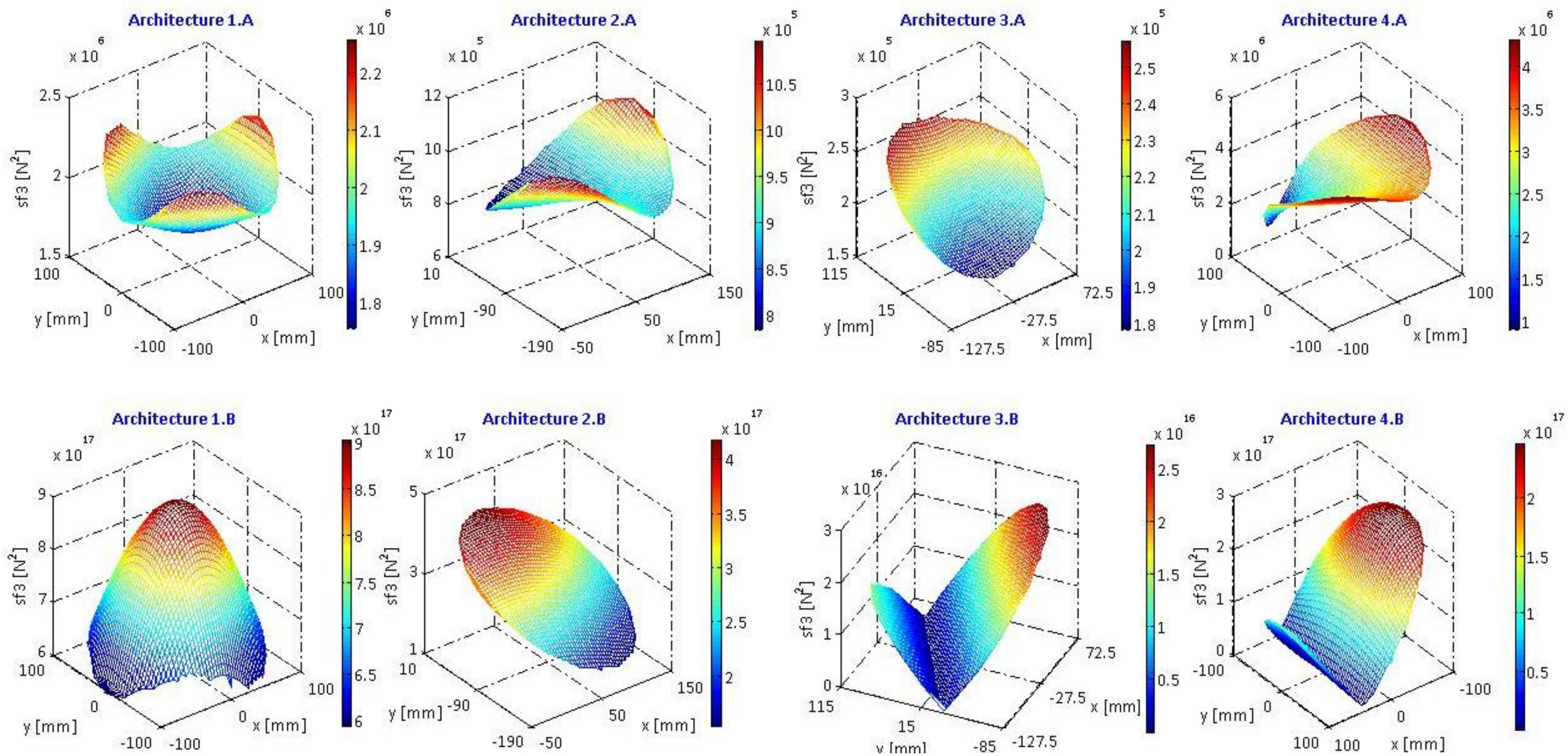

Figure 4.4. *Distribution of the stiffness index sf_3 in the section W of the workspace for each architecture of the 3-UPU TPM*

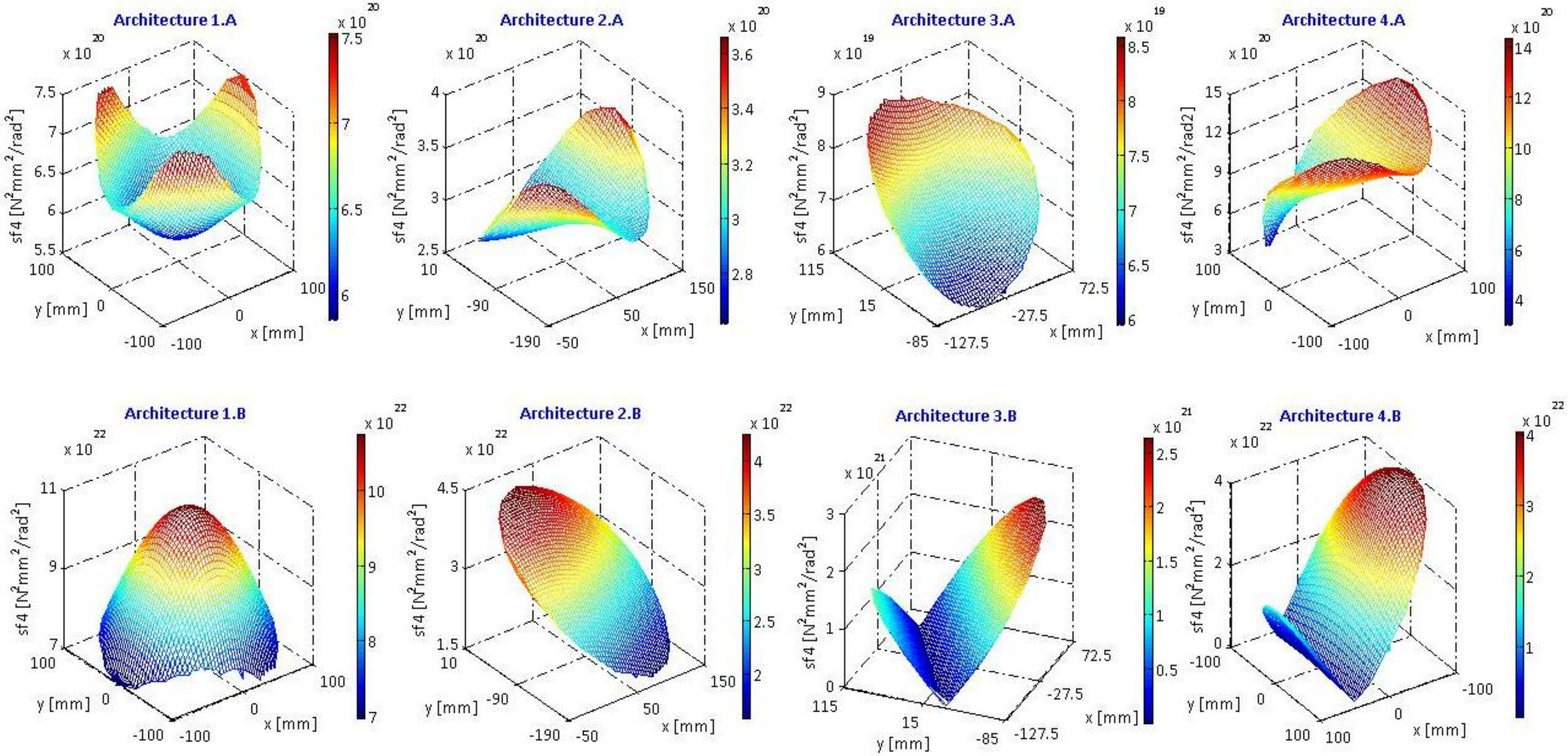

Figure 4.5. *Distribution of the stiffness index sf_4 in the section W of the workspace for each architecture of the 3-UPU TPM*

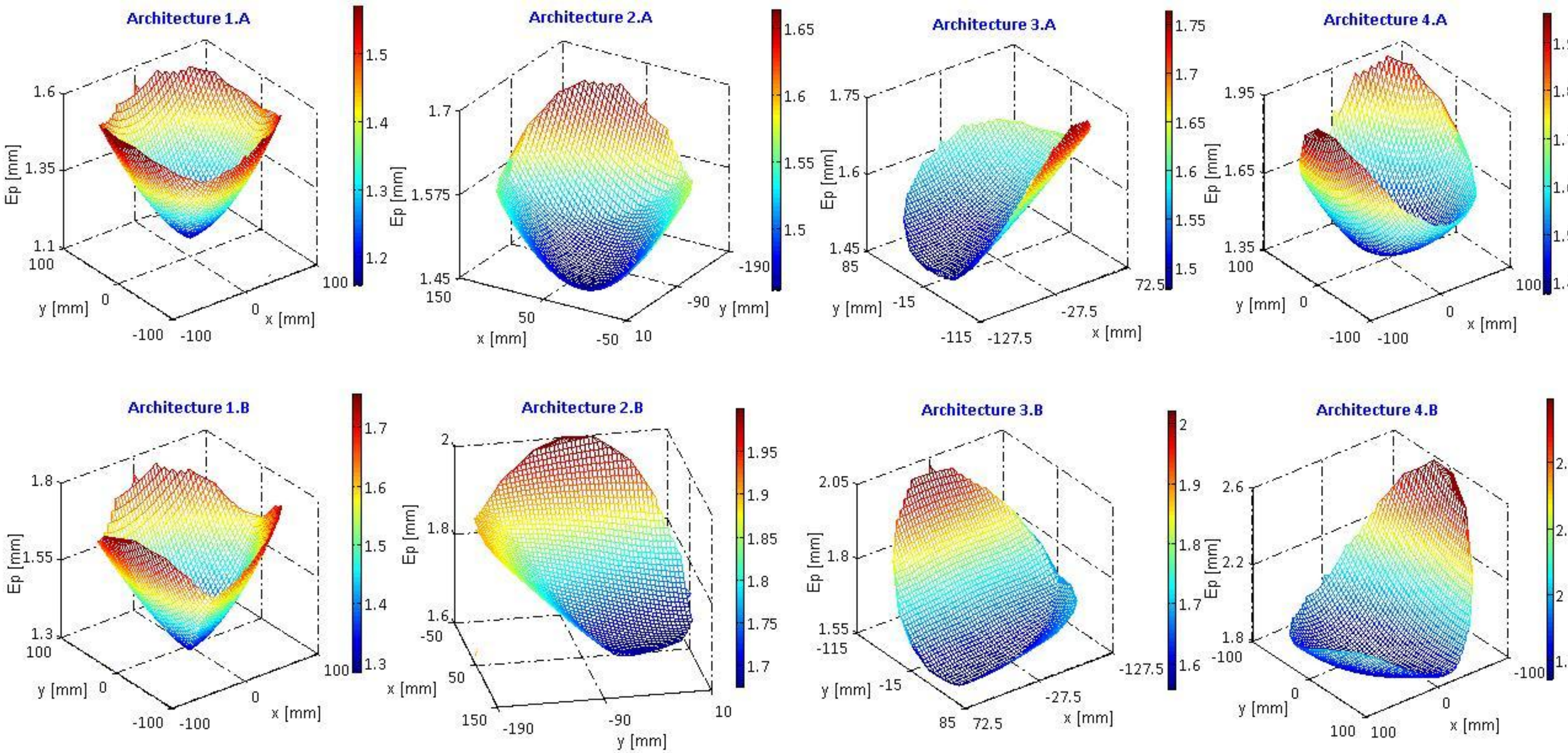

Figure 4.6. *Distribution of the maximum of the platform position error E_p in the section W of the workspace for each architecture of the 3-UPU TPM*

Conclusion

This dissertation recalls the most relevant features of the 3-UPU TPMs, a very well know 3-DOF translational parallel manipulator presented in the literature in the late nineties by Tsai [4].

Investigation of the influence of both the directions of the base/platform revolute joints axes and the leg position is further investigated and six new architectures of the manipulator which exhibit interesting performances are presented. Moreover, three manufacturing solutions are proposed for the leg collision avoidance of the architecture that feature a crossed leg pattern of the 3-UPU TPM.

A procedure to select the best architecture of the 3-UPU TPMs among a number of them for a given task has been presented. The procedure is based on a number of indexes which correspond to the singularity loci, the size of the manipulator, the stiffness of the manipulator (taken as the determinants of the 3x3 matrices obtained by partitioning of the stiffness matrix, that relates the external wrench applied to the platform to the displacement of the platform itself) and the maximum value of the platform position error due to the axial and radial clearance in the revolute joints.

Finally, a case study is reported for the application of the procedure. The selection of the optimal architecture of the manipulator is done in two ways. The first one is based on each individual index. For this selection, the best architecture changes according to the index. The second selection is based on an objective function which corresponds to a proper weighted selection of the different indexes. According to this selection, one of the 3-UPU architecture that features a crossed leg pattern has found to be the best, i.e. the one that corresponds to the maximum value of the defined objective function.

Bibliography

[1] Clavel, R., 1988. "Delta, a fast robot with parallel geometry". *In 18th Int. Symp. On Industrial Robots*, pp. 91-100, April 26-28, Lausanne.

[2] Hervè, J.M., Sparacino, F., 1991. "Structural synthesis of parallel robots generating spatial translation". *Fifth ICAR International Conference on Advanced Robotics*, pp. 808-813, June 19–22, Pisa, Italy.

[3] Hervè, J.M., 1992. "Group mathematics and parallel link mechanisms". *In: Proceedings of the IMACS SICE International Symposium on Robotics, Mechatronics and Manufacturing Systems*, pp. 459–464, Kobe, Japan.

[4] Tsai, L.W., 1996. "Kinematics of three-degrees of freedom platform with three extensible limbs". *Recent advances in robot kinematics, Kluwer*, pp. 401-410, Dordrecht, Netherlands.

[5] Tsai, L.W. and Stamper, R., 1996. "A parallel manipulator with only translational degrees of freedom", *In: ASME 96-DETC-MECH-1152*, Irvine, CA, USA.

[6] Parenti-Castelli, V., Bubani, F., 1999. "Singularity Loci and Dimensional Design of a Translation 3-dof Fully-Parallel manipulator". *Proceedings of Advances in Multibody Systems and Mechatronics,* pp. 319-332, Duisburg, Germany.

[7] Parenti-Castelli, V., Di Gregorio, R., Bubani, F., 2000. "Workspace and Optimal Design of a Pure Translation Parallel Manipulator". *Meccanica*, vol. 35, pp. 203–214.

[8] Parenti-Castelli, V., Di Gregorio, R., 2000. "Influence of the manufacturing errors on the kinematic performances of the 3-UPU parallel mechanism". *2nd Chemnitz Parallel Kinematics Seminar - Working Accuracy of Parallel Kinematics*, pp. 85-100.

[9] Di Gregorio, R., Parenti-Castelli, V., 2002. "Mobility analysis of the 3-UPU parallel mechanism assembled for a pure translational motion". *ASME Transactions, Journal of Mechanical Design*, vol. 124, pp. 259-264.

[10] Tsai, L.W., Joshi, S., 2002. “Kinematics analysis of 3-DOF position mechanisms for use in hybrid kinematic machines”. *ASME Transactions, Journal of Mechanical Design*, vol. 124, pp. 245-253.

[11] Gosselin, L., Angeles, J., 1989. “The optimum kinematic design of a spherical three-degree-of-freedom parallel manipulator”. *ASME Journal of Mechanisms, Transmission and Automation in Design*, vol. 111, pp. 202-207.

[12] Di Gregorio, R., Parenti-Castelli, V., 1999. “Influence of the geometric parameters of the 3-UPU parallel manipulator on the singularity loci”. *PKM99, Parallel Kinematic Machines, International Workshop on parallel machines*, Milan, Italy.

[13] Kong, X., Gosselin, C., 2004. “Type Synthesis of 3-DOF Translational Parallel Manipulators Based on Screw Theory”. *Journal of Mechanical Design, Transactions of the ASME*, vol. 126, pp. 83-92.

[14] Zlatanov, D., Bonev, I.A., and Gosselin, C., 2002. “Constraint singularities of parallel mechanisms”. *Proceedings - IEEE International Conference on Robotics and Automation*, vol. 1, pp. 496-502.

[15] G. Gogu, Structural Synthesis of Parallel Robots - Part 2: Translational Topologies with Two and Three Degrees of Freedom, Series: Solid Mechanics and Its Applications, vol. 159, 2009, XVIII, 762 p., ISBN: 978-1-4020-9793-5.

[16] Chebbi, A.H., Parenti-Castelli, V., Romdhane, L., 2009. “Optimal Design of a Pure Translation Manipulator with clearance joints”. *CMSM 2009, March 16-18, Hammamet*, Tunisia.

[17] Di Gregorio, R., Parenti-Castelli, V., 1998. “A Translational 3-DOF Parallel Manipulator”. *Advances in Robot Kinematics: Analysis and Control*, pp. 49-58.

[18] Yang Po-hua, K., Waldron, D.E. Orin, 1996. “Kinematic of a three-degree-of-freedom motion platform for a low-cost driving simulator”, *Advances in Robot Kinematics, Kluwer Academic Publishers*, pp. 89-98.

[19] Kong, X., Gosselin, C., 2007. Type Synthesis Of Parallel Mechanisms, Springer London Publisher, 272 p, ISBN: 9783540719892.

[20] Walter, D.R., Husty, M.L., and Pfurner, M., 2008. "The SNU 3-UPU Parallel Robot from a Theoretical Viewpoint". *Proceedings of the Second International Workshop on Fundamental Issues and Future Research Directions for Parallel Mechanisms and Manipulators*, pp. 1-8, Montpellier, France.

[21] Walter, D.R., Husty, M.L., and Pfurner, M., 2009. "A Complete Kinematic Analysis of the SNU 3-UPU Parallel Robot". *Contemporary Mathematics, American Mathematical Society*, vol. 496, pp. 331-346.

[22] Wolf, A., Shoham, M., 2006. "Screw theory tools for the synthesis of the geometry of a parallel robot for a given instantaneous task". *Mechanism and Machine Theory*, vol. 41, pp. 656-670.

[23] Chebbi, A.H., Parenti-Castelli, V., 2010. "Influence of the geometry on the performances of the 3-UPU parallel manipulator". *3-rd European Conference on Mechanism Science EUCOMES 2010*, pp. 595-603, 14-18 September, Cluj-Napoca, Romania

[24] Chebbi, A.H., Parenti-Castelli, V., 2010. "Potential of the 3-UPU Translational Parallel Manipulator". Proceeding of ASME 2010 International Design Engineering Technical Conferences & Computers and Information in Engineering Conference IDETC/CIE 2010, 15-18 August, Montreal, Canada.

[25] Hartenberg, R.S., Denavit, J., Kinematic synthesis of linkages, McGraw-Hill Education Publisher, 1964, 435 p., ISBN: 9780070269101.

[26] John J. Craig, Introduction to robotics mechanics and control: Second Edition, Addison-Wesley Publishing Company, 1989, 450 p., ISBN: 0-201-09528-9

[27] Duffy, J., 1990. "The Fallacy of Modern Hybrid Control Theory that is Based on 'Orthogonal Complements' of twist and Wrench Spaces". *Journal of Robotic Systems*, vol. 7, pp. 139-144.

[28] Pashkevich, A., Chablat, D., Wenger, P., 2009. "Stiffness analysis of overconstrained parallel manipulators". *Mechanism and Machine Theory*, vol. 44, pp. 966–982.

[29] C. Innocenti, C., 2002. "Kinematic clearance sensitivity analysis of spatial structures with revolute joints". *ASME Journal of Mechanical Design*, vol. 124, pp. 487–496.

[30] Parenti-Castelli, V., Venanzi, S., 2005. “Clearance influence analysis on mechanisms”. *Mechanism and Machine Theory*, vol. 40, pp. 1316–1329.

[31] Chebbi, A.H., Affi, Z., Romdhane, L., 2009. “Prediction of the pose errors produced by joints clearance for a 3-UPU parallel robot”. *Mechanism and Machine Theory*, vol. 44, pp. 1768–1783.

[32] Venanzi, S., Parenti-Castelli, V., 2005. “A new technique for clearance influence analysis in spatial mechanisms”. *ASME Journal of Mechanical Design*, vol. 127, pp. 446–455.

[33] Venanzi, S., 2004. “Methods for Clearance Influence Analysis in Planar and Spatial Mechanisms”. *Ph.D. dissertation*, University of Bologna, Bologna, Italy.

[34] Innocenti, C., 1999. ”A Static-Based Method to Evaluate the Effect of Joint Clearances on the Positioning Errors of Planar Mechanisms”. *Proceedings of the 10th World Congress on the Theory of Machines and Mechanisms*, Oulu, Finland, pp. 650 - 655.

[35] Innocenti, C., 1999. ”Kinematic Clearance Sensitivity Analysis of Spatial Structures with Revolute Joints”. *Proceedings of the 1999 ASME Design Engineering Technical Conference*, Las Vegas, USA.

[36] Parenti-Castelli, V., and Venanzi, S. 2002. ”A New Deterministic Method for Clearance Influence Analysis in Spatial Mechanisms”. *Proceedings of the 2002 ASME International Mechanical Engineering Congress and Exposition*, New Orleans, USA.

[37] Matlab Company. Matlab user guide: version 7.9. USA: Matlab Company; 2009.

Appendix A

The full expression of the coefficients A, B, D, E and F are the following:

$$A = \kappa_{11}\kappa_{12}\left(\lambda_{11}^{2} + \lambda_{12}^{2}\right) - \lambda_{11}\lambda_{12}\left(\kappa_{11}^{2} + \kappa_{12}^{2}\right) \tag{A.1}$$

$$B = 2\left(\lambda_{11}^{2}\kappa_{12}^{2} - \kappa_{11}^{2}\lambda_{12}^{2}\right) \tag{A.2}$$

$$D = -(b-p)\left(\frac{\kappa_{11}\left(\lambda_{11}^{2} + \lambda_{12}^{2}\right)\left(\sqrt{3}\kappa_{11} + \kappa_{12}\right)}{2} + \lambda_{11}\lambda_{12}\left(\kappa_{11}^{2} + \kappa_{12}^{2}\right)\right) \tag{A.3}$$

$$E = -(b-p)\left(\frac{\sqrt{3}\kappa_{11}\kappa_{12}\left(\lambda_{11}^{2} + \lambda_{12}^{2}\right)}{2} + \frac{3\kappa_{12}^{2}\lambda_{12}^{2}}{2} + \frac{\lambda_{11}^{2}\kappa_{12}^{2}}{2} + \kappa_{11}^{2}\lambda_{12}^{2}\right) \tag{A.4}$$

$$F = -(b-p)^{2}\left(\frac{\left(\lambda_{11}^{2} + \lambda_{12}^{2}\right)\left(2\kappa_{11}\kappa_{12} + 3\sqrt{3}\kappa_{12}^{2} + \sqrt{3}\kappa_{11}^{2}\right)}{4} + \lambda_{11}\lambda_{12}\left(\kappa_{11}^{2} + \kappa_{12}^{2}\right)\right) \tag{A.5}$$

where κ_{11}, λ_{11}, κ_{12} and λ_{12} are respectively the x and y components of the unit vectors $\mathbf{q}_{11}$ and $\mathbf{q}_{12}$ in the system S_b.

Appendix B

The routine used in order to obtain the relation given by Eqn. (3.20) is the following: the expression of the unit vector $\mathbf{q}_{2i}$, i = 1,2,3, of the direction of the intermediate revolute joint of the i-th leg is given by:

$$\mathbf{q}_{2i} = \frac{\mathbf{q}_{1i} \times \mathbf{s}_i}{\|\mathbf{q}_{1i} \times \mathbf{s}_i\|} = \frac{\mathbf{q}_{1i} \times \mathbf{s}_i}{|\sin\omega_i|} \qquad i = 1,2,3 \tag{B.1}$$

where $\mathbf{s}_i$, is the unit vector of the i-th leg; $\mathbf{q}_{1i}$, is the unit vector of the direction of the revolute joint that connect the i-th leg to the base and ω_i is the angle formed by the two unit vectors $\mathbf{s}_i$ and $\mathbf{q}_{1i}$.

The unit vector $\mathbf{u}_i$, i = 1,2,3, of the direction orthogonal to the cross link of the universal joint is expressed as:

$$\mathbf{u}_i = \mathbf{q}_{1i} \times \mathbf{q}_{2i} = \frac{\mathbf{q}_{1i} \times (\mathbf{q}_{1i} \times \mathbf{s}_i)}{|\sin\omega_i|} = \frac{(\mathbf{q}_{1i}.\mathbf{s}_i).\mathbf{q}_{1i} - (\mathbf{q}_{1i}.\mathbf{q}_{1i}).\mathbf{s}_i}{|\sin\omega_i|} = \frac{\cos\omega_i\,\mathbf{q}_{1i} - \mathbf{s}_i}{|\sin\omega_i|} \qquad i = 1,2,3 \tag{B.2}$$

By using the expression of the unit vectors $\mathbf{u}_i$, i = 1,2,3, given by the previous equation, the scalar product of the two unit vectors $\mathbf{s}_i$ and $\mathbf{u}_i$, i = 1,2,3, which corresponds to the cosine of the angle φ_i (formed by these unit vectors), is given as follows:

$$\mathbf{u}_i.\mathbf{s}_i = \frac{\cos\omega_i(\mathbf{q}_{1i}.\mathbf{s}_i) - (\mathbf{s}_i.\mathbf{s}_i)}{|\sin\omega_i|} = \frac{\cos^2\omega_i - 1}{|\sin\omega_i|} = \pm\sin\omega_i \quad i = 1,2,3 \tag{B.3}$$

Thus, the relation between the two angles ω_i and φ_i, is given by:

$$\cos\varphi_i = \pm\sin\omega_i \qquad i = 1,2,3 \tag{B.4}$$

Thus, the absolute value of the rate μ_i, i = 1,2,3, between the bending moment m_{bi}, and the torque m_{ti}, acting on the i-th leg is expressed as:

$$|\mu_i| = \left|\frac{\cos\omega_i}{\sin\omega_i}\right| \qquad i = 1,2,3 \tag{B.5}$$

The expression of the matrices $\mathbf{W}_{1,ji}$, $\mathbf{W}_{2,ji}$ and $\mathbf{W}_{3,ji}$, i = 1,2,3; j = 1,2,3,4, are given as follows:

$$\mathbf{W}_{1,ji} = \begin{bmatrix} \frac{\eta_{ji}^2+\lambda_{ji}^2}{2} & -\frac{\kappa_{ji}\lambda_{ji}}{2} & -\frac{\kappa_{ji}\eta_{ji}}{2} & 0 & -\frac{\eta_{ji}}{2L} & \frac{\lambda_{ji}}{2L} \\ -\frac{\kappa_{ji}\lambda_{ji}}{2} & \frac{\kappa_{ji}^2+\eta_{ji}^2}{2} & -\frac{\lambda_{ji}\eta_{ji}}{2} & \frac{\eta_{ji}}{2L} & 0 & -\frac{\kappa_{ji}}{2L} \\ -\frac{\kappa_{ji}\eta_{ji}}{2} & -\frac{\lambda_{ji}\eta_{ji}}{2} & \frac{\lambda_{ji}^2+\kappa_{ji}^2}{2} & -\frac{\lambda_{ji}}{2L} & \frac{\kappa_{ji}}{2L} & 0 \end{bmatrix} \tag{B.6}$$

$$\mathbf{W}_{2,ji} = \begin{bmatrix} \frac{\eta_{ji}^2+\lambda_{ji}^2}{2} & -\frac{\kappa_{ji}\lambda_{ji}}{2} & -\frac{\kappa_{ji}\eta_{ji}}{2} & 0 & \frac{\eta_{ji}}{2L} & -\frac{\lambda_{ji}}{2L} \\ -\frac{\kappa_{ji}\lambda_{ji}}{2} & \frac{\kappa_{ji}^2+\eta_{ji}^2}{2} & -\frac{\lambda_{ji}\eta_{ji}}{2} & -\frac{\eta_{ji}}{2L} & 0 & \frac{\kappa_{ji}}{2L} \\ -\frac{\kappa_{ji}\eta_{ji}}{2} & -\frac{\lambda_{ji}\eta_{ji}}{2} & \frac{\lambda_{ji}^2+\kappa_{ji}^2}{2} & \frac{\lambda_{ji}}{2L} & -\frac{\kappa_{ji}}{2L} & 0 \end{bmatrix} \tag{B.7}$$

$$\mathbf{W}_{3,ij} = \begin{bmatrix} \kappa_{ji} & \lambda_{ji} & \eta_{ji} & 0 & 0 & 0 \end{bmatrix} \tag{B.8}$$

where:

κ_{ji}, λ_{ji} and η_{ji}, i = 1,2,3; j = 1,2,3,4, are respectively the x, y and z components of the unit vector $\mathbf{q}_{ji}$ of the j-th revolute joint connected to the i-th leg; L is the half of the axial length of the revolute joints.